A semi-analytical model of the influence of phytoplankton community structure on the relationship between light attenuation and ocean color

Áurea M. Ciotti, John J. Cullen, and Marlon R. Lewis

Centre for Environmental Observation Technology and Research, Department of Oceanography, Dalhousie University, Halifax, Nova Scotia, Canada

Abstract. A model was developed to examine the influence of phytoplankton community structure on the relationship between diffuse attenuation and ratios of upwelling radiance. Shifts in phytoplankton communities were represented by changing mean optical properties as a function of chlorophyll (C, mg m^{-3}), consistent with large data sets from the field and laboratory. The product of cell size and internal pigment concentration, dc_i, governs pigment packaging, which alters the specific absorption coefficients of phytoplankton (a^*_{ph}, m^2 mgChl^{-1}). Pigment packaging was parameterized as a function of C by combining the relationship between dc_i and a^*_{ph} from phytoplankton cultures with that between a^*_{ph} and C from the field, using data for 675 nm, where absorption by accessory pigments is low. Changes in accessory pigmentation were approximated by quantifying residual variability in a^*_{ph} at other wavelengths, as functions of C, once the variability with dc_i was taken into account. Absorption by colored dissolved organic matter (CDOM), detrital absorption, and scattering by particles were also parameterized as functions of C, so that bio-optical relationships could be modeled as functions of trophic status. The model thus reconciled recognized relationships between optical properties and C with ecologically interpretable shifts in phytoplankton communities. Empirical relationships between diffuse attenuation and ocean color were well reproduced at low (0.5 mg m^{-3}) to medium (10 mg m^{-3}) C. Analysis of variability imposed by a range of dc_i suggests that it may be possible to recognize phytoplankton communities with cell sizes and intracellular pigment concentration different from the central tendency, given a set of wavelengths which minimizes the influence of CDOM and detrital absorption.

1. Introduction

Understanding the factors controlling the attenuation of solar energy in the ocean is of central importance in oceanography, as attenuation influences photosynthetic rates [e.g. *Platt et al.*, 1988], photochemistry [e.g., *Miller*, 1994], and upper ocean thermal dynamics [e.g., *Lewis et al.*, 1990]. Robust empirical relationships derived from regressions of attenuation on ocean color measurements [e.g., *Aarup et al.*, 1996; *Austin and Petzold*, 1981; *Mueller and Trees*, 1997] make feasible the use of ocean color drifters and remotely sensed observations to estimate attenuation in surface waters. The robust relationship between ocean color and attenuation reflects fundamental physical and biological bases that deserve further investigation. Explicit representation of the terms in these relationships allows a transition from an empirical approach for prediction to a more rigorous analytical foundation [*Gordon et al.*, 1988] which permits the quantitative exploration of the role of various dissolved and particulate components on its variability. This is achieved by parameterizing the optical properties that govern both attenuation and ocean color, that is, absorption and scattering.

In most oceanic situations, the attenuation of light is strongly affected by biogenic particles, such as phytoplankton. In coastal waters the parameterization of both absorption and scattering is complicated by the presence of inorganic particles and colored dissolved organic matter (CDOM), and by variability in species composition of phytoplankton. Our approach was to develop a model that explained the central tendency for both absorption and backscattering coefficients to vary with C, in terms of ecologically interpretable shifts in phytoplankton communities from oligotrophic to eutrophic environments [see *Yentsch and Phinney*, 1989]. The basis of the parameterization was a large data set of optical measurements from both field and laboratory investigations; the influences of pigment packaging and changes in pigment composition on phytoplankton absorption were considered independently. The influences of detrital and CDOM optical properties were also included in the model.

The resulting model therefore reconciles a wide range of known relationships between optical properties and trophic status, along with theoretical relationships and data from field and laboratory, so that the optical consequences of changes in phytoplankton community structure can be assessed. The model explains a large fraction of the variability in relationships between ocean color and diffuse attenuation, as well as most of the variability in a relationship between ocean color and bulk chlorophyll concentration using remote

sensing techniques (i.e., radiance ratios). The semi-analytical nature of the model lets us examine several types of residual variation about the central tendency, associated with changes in cell size (pigment packaging) and in pigment composition, as well as with detritus and CDOM. Analysis of this residual variability allows us to assess the influence of local phytoplankton communities on optical relationships in coastal waters. In turn, the model can be used to interpret deviations in relationships between optical properties as expressions of different phytoplankton communities. The model is thus a useful tool to understand the extend to which variable optical properties reflect ecological dynamics in coastal waters.

2. Background

Both the diffuse attenuation coefficient and radiance ratios are so-called apparent optical properties (AOPs) which depend on both the optical properties of the water and its constituents, and the geometrical distribution of the radiance field [*Preisendorfer*, 1961]. A parameterization of the relationship between attenuation and upwelling radiance ratios from first principles requires that this relationship be described using inherent optical properties (IOPs) only, which are independent of the radiance field. It is noteworthy that comparisons between two AOPs will be influenced by changes in the geometrical distribution of the radiance. Nevertheless, because we are comparing the attenuation coefficient, which can be treated as a quasi-inherent optical property [*Preisendorfer*, 1961], to ratios of upwelling radiance, for which the parameters describing the geometric distribution of radiance largely cancel out (see below), the effects of changes in the light field in our comparison are expected to be small.

2.1. Ratios of spectral radiance at the surface

Surface irradiance reflectance ($R(\lambda)$, dimensionless, see Notation) is defined as the ratio of upwelling to downwelling irradiance just below the surface. Relationships between $R(\lambda)$ and IOPs are well known [see *Gordon et al.*, 1988, and references therein].

$$R(\lambda) = \frac{E_u(\lambda)}{E_d(\lambda)} = \frac{Q(\lambda)L_u(\lambda)}{E_d(\lambda)} \approx f(\lambda)\frac{b_b(\lambda)}{a(\lambda)+b_b(\lambda)}, \qquad (1)$$

where $E_u(\lambda)$ and $E_d(\lambda)$ are the upwelling and downwelling spectral irradiances (W m^{-2} nm^{-1}), $L_u(\lambda)$ is the upwelling radiance (W m^{-2} nm^{-1}sr^{-1}), $Q(\lambda)$ is the ratio of the upwelling irradiance to the nadir upwelling radiance (sr), $f(\lambda)$ is a parameter that depends on the geometrical distribution of the light field (dimensionless), $a(\lambda)$ is the total absorption coefficient (m^{-1}), and $b_b(\lambda)$ is the total backscattering coefficient (m^{-1}). It is important to note that while both $f(\lambda)$ and $Q(\lambda)$ vary primarily with changes in the local radiance distribution, they are also functions of the water constituents [e.g., *Morel and Gentili*, 1996].

Given two wavelengths, λ_1 and λ_2, their radiance ratio can be expressed as

$$\frac{L_u(\lambda_1)}{L_u(\lambda_2)} = \left(\frac{f(\lambda_1)b_b(\lambda_1)E_d(\lambda_1)}{Q(\lambda_1)(a(\lambda_1)+b_b(\lambda_1))}\right)\left(\frac{Q(\lambda_2)(a(\lambda_2)+b_b(\lambda_2))}{f(\lambda_2)b_b(\lambda_2)E_d(\lambda_2)}\right). \qquad (2)$$

For consistency with previous work, and with no loss of

generality, we choose two specific wavelengths, 443 and 550 nm. Equation (2) can be further simplified if it is assumed that $b_b \ll a$ [*Gordon et al.*, 1988; *Morel and Prieur*, 1977]:

$$\frac{L_u(443)}{L_u(550)} = \left(\frac{f(443)/Q(443)}{f(550)/Q(550)}\right)\left(\frac{E_d(443)}{E_d(550)}\right)\left(\frac{b_b(443)a(550)}{b_b(550)a(443)}\right). \qquad (3)$$

This assumption will not be valid in highly turbid environments, which are outside of the scope of this paper [see *Kirk*, 1994a]. We can group the first two terms in (3), so that

$$\left(\frac{f(443)/Q(443)}{f(550)/Q(550)}\right)\left(\frac{E_d(443)}{E_d(550)}\right) = M. \qquad (4)$$

The value of M can, in principle, be computed by assuming a spectral shape for $E_d(\lambda)$ and estimating the spectral dependence of $f(\lambda)/Q(\lambda)$. The spectral shape of $E_d(\lambda)$ can be measured easily, or computed using a clear sky model in which the inputs are atmospheric conditions, solar angle, and surface albedo [*Gregg and Carder*, 1990]. For a variety of parameters within the expected ranges for our experiments, several runs of the clear sky model by *Gregg and Carder* [1990] generated values of $E_d(443)/E_d(550)$ between 0.92 and 0.98, with a median value of 0.95. Both $f(\lambda)$ and $Q(\lambda)$ are functions of the geometrical distribution of radiance and of the IOPs, as mentioned before. However, for Case 1 waters with chlorophyll concentrations below 3 mg m^{-3}, Monte Carlo simulations [*Morel and Gentili*, 1993] have shown that the relationship between $f(443)/Q(443)$ and $f(550)/Q(550)$ obeys a one-to-one ratio with an error of ±3.5%. We will assume that this one-to-one ratio is valid in our parameterization, but increasing variability is expected as chlorophyll increases [*Morel and Gentili*, 1996]. For simplicity, we will initially consider M to be equal to 0.95, representing an "expected" value of $E_d(443)/E_d(550)$, so that (3) becomes

$$\frac{L_u(443)}{L_u(550)} = 0.95\frac{b_b(443)a(550)}{b_b(550)a(443)}. \qquad (5)$$

Throughout this paper we will refer always to 550 nm for the green wave band, even when field data are for slightly different wavelengths (see Results). As will be shown later, both optical and biological data are weighted by the wavelength responses of the sensors, but in the green region, gradients with respect to wavelength are small. Thus at a first approximation the differences among the instruments used and modeled relationships can be ignored.

2.2 Diffuse Attenuation Coefficient

The diffuse vertical attenuation coefficient $K_d(\lambda)$ (m^{-1}) can be also described as a function of IOPs [e.g., *Gordon et al.*, 1975; *Sathyendranath and Platt*, 1988]:

$$K_d(\lambda) = \frac{a(\lambda) + b_b(\lambda)}{\bar{\mu}_d(\lambda)}, \qquad (6)$$

where $\bar{\mu}_d(\lambda)$ is the average cosine for downwelling irradiance, defined as the ratio of $E_d(\lambda)$ to $E_0(\lambda)$, the downwelling scalar irradiance. The value of $\bar{\mu}_d(\lambda)$ is influenced by the angular distribution of the incident radiance, changing with solar angle and with the proportions of diffuse to direct light

[*Bukata et al.*, 1995]. The average cosine is also a function of the ratio between the scattering and absorption coefficients (*b/a*) for a given solar angle [*Kirk*, 1994b, and references therein]; it will therefore change with different particle assemblages. Assuming fixed solar angles between vertically incident and 45°, and *b/a* ranging from 2 to 15 (coastal waters), $\bar{\mu}_d$ varies from approximately 0.75 to 0.65 [*Kirk*, 1994b]. Thus we will assume a constant value of 0.7 for $\bar{\mu}_d$. This assumption may not hold for waters with very small *b/a* (low particles and high CDOM concentration), but because we are interested mainly in coastal waters, we feel that this assumption will hold for the situations analyzed in this work. In fact, for a time series of measurements collected in Bedford Basin (described below), the relationship between $K_d(\lambda)$ in the blue and green regions and total absorption coefficient (not shown) was linear (r^2=0.79) with a slope of 0.713 (± 0.035) consistent with our assumed value for $\bar{\mu}_d$.

3. Model Structure and Parameterization of IOPs

Equations (5) and (6) show that the IOPs necessary to reproduce the relationship between $K_d(490)$ and $L_u(443)/L_u(550)$ are the total absorption coefficients ($a(\lambda)$) and the total backscattering coefficients ($b_b(\lambda)$) at 443, 490, and 550 nm. The constituents that govern the variability in IOPs are generally divided into four groups [see *Kirk*, 1994b]: water (w), phytoplankton (ph), CDOM, and particles other than phytoplankton, hereinafter referred to as detritus (det). In the following sections, we will describe the parameterization of these IOPs with trophic status, represented by concentration of chlorophyll plus pheopigments (*C*, mg m⁻³). Pheopigments are assumed to be unimportant, as our analysis is focused on surface waters, where the lifetime of pheopigments is short [*SooHoo and Kiefer*, 1982]. A schematic representation of the steps for the development of the model is presented in Figure 1.

3.1. Total Absorption

IOPs are additive, so that, following the abbreviations described above:

$$a(\lambda) = a_w(\lambda) + a_{ph}(\lambda) + a_{cdom}(\lambda) + a_{det}(\lambda). \tag{7}$$

The absorption coefficients for seawater are assumed to be constant and equal to those for pure water [*Pope and Fry*, 1997]. The other components will be parameterized as a function of *C*, as described below.

3.1.1. Parameterization of phytoplankton absorption. Phytoplankton absorption is usually represented as

$$a_{ph}(\lambda) = C\, a^*_{ph}(\lambda), \tag{8}$$

where $a^*_{ph}(\lambda)$ (m² mg Chl⁻¹) is the chlorophyll-specific absorption coefficient of phytoplankton. Changes in cell size and in the composition and degree of packaging of pigments influence $a^*_{ph}(\lambda)$ [*Babin et al.*, 1993; *Bricaud et al.*, 1995; *Bricaud et al.*, 1983; *Morel and Bricaud*, 1981; *Nelson et al.*, 1993; *Sathyendranath et al.*, 1987; *Sosik and Mitchell*, 1995; *Stuart et al.*, 1998; *Yentsch and Phinney*, 1989]. Thus $a^*_{ph}(\lambda)$ is not constant and has been parameterized as a function of *C* by assuming diverse forms for the relationship between $a_{ph}(\lambda)$ and *C* (see discussion by *Lutz et al.* (1996)).

When analyzed in the context of trophic status, changes in both spectral shape and amplitude of $a^*_{ph}(\lambda)$ are associated with changes in community structure. An extensive set of data is now available for $a^*_{ph}(\lambda)$ covering *C* from 0.02 to 25 mg m⁻³ [*Bricaud et al.*, 1995]. We have used the near-surface portion of these data (A. Bricaud, personal communication, 1997) and our data collected off the Oregon coast [*Ciotti et al.*, 1996] and in a coastal embayment (Bedford Basin, Nova Scotia, Canada) to develop an approximation for packaging and pigment composition, each as a function of *C*. To minimize the effects of photoacclimation on $a^*_{ph}(\lambda)$, only data from the first optical depth were used [*Mitchell*, 1992]. These data correspond to particulate absorption, corrected for the absorption by detritus and normalized by the concentration of chlorophyll plus pheopigments. The optical depth (for 490 nm) was estimated from *C* following *Morel* [1988] when direct measurements of $K_d(490)$ were not available.

3.1.1.1. Packaging. The packaging effect [*Kirk*, 1994b] comes from the intracellular self-shading which lowers $a^*_{ph}(\lambda)$ and flattens the absorption spectra [*Duysens*, 1956]. It is well known that $a^*_{ph}(\lambda)$ decreases as *C* increases as a result of increasing packaging [*Bricaud et al.*, 1995, and references therein], which is mainly controlled by the cell size, or diameter (*d*), and the intracellular concentration of pigments, c_i [*Bricaud and Morel*, 1986; *Sathyendranath et al.*, 1987]. In what follows, we will develop an approximation for the product of the diameter and the intracellular pigment concentration (dc_i) as a function of *C*.

Ideally, we should parameterize dc_i versus *C* following first principles of physiological ecology and cell optics, using a characterization of changes in phytoplankton communities as *C* increases [cf. *Yentsch and Phinney*, 1989]. We have simplified the *Yentsch and Phinney* [1989] approach by representing whole communities with an average dc_i that varies as a function of *C*. These average cells have the mean optical properties of the entire community (but see *Campbell* [1995] for a quantitative analysis of this assumption for phytoplankton absorption).

Once whole phytoplankton communities are characterized as average cells, their optical properties can be estimated within the framework of the anomalous diffraction approximation [*van de Hulst*, 1957] if it is assumed that these average cells are randomly distributed with respect to the light field, and that they behave as homogeneous spherical particles [*Morel and Bricaud*, 1986]. The efficiency factor for absorption ($Q_a(\lambda)$; dimensionless) for a single phytoplankton cell, that is, the ratio of absorbed to impinged energy on the geometrical cross section of the cell, can be estimated as

$$Q_a(\lambda) = 1 + \frac{2e^{(-\rho'(\lambda))}}{\rho'(\lambda)} + 2\left(\frac{e^{(-\rho'(\lambda))} - 1}{\rho'(\lambda)^2}\right), \tag{9}$$

where $\rho'(\lambda)$ is the dimensionless optical thickness of the particle. This is defined as the product of three quantities: the specific absorption coefficient of the cellular material as in solution ($a^*_{sol}(\lambda)$; m² mgChl⁻¹), the intracellular concentration of this material (c_i mg m⁻³) and the cell diameter (*d*; meters), that is,

$$\rho'(\lambda) = a^*_{sol}(\lambda) dc_i. \tag{10}$$
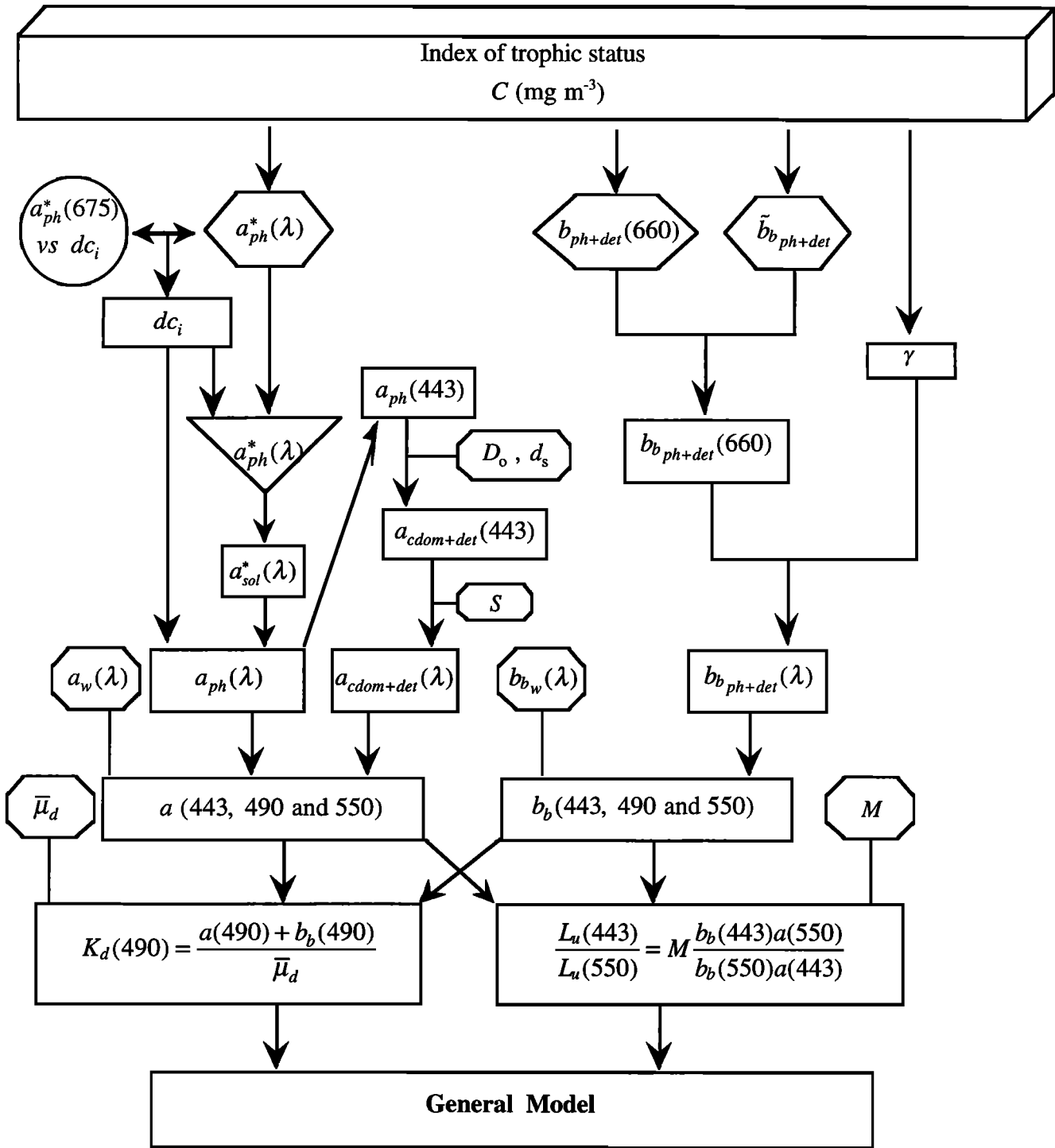
Figure 1.

Note that the only quantity that varies spectrally in (10) is $a^*_{Sol}(\lambda)$.

We now relate this theoretical absorption efficiency to the variability in $a^*_{ph}(\lambda)$ observed in the field. To isolate the effect of the packaging (expressed as dc_i) on $a^*_{ph}(\lambda)$ from the effect of accessory pigments (hereinafter referred to as "pigment composition"), we will look at a wavelength where the absorption by accessory pigments is not important. At 675 nm, phytoplankton absorption is due almost exclusively to chlorophyll a [Bidigare et al., 1990], so a constant value for $a^*_{Sol}(675)$, independent of pigment composition, can be assumed.

A coefficient representing the degree of pigment packaging is determined as follows:

$$Q^*_a(\lambda) = \frac{a^*_{ph}(\lambda)}{a^*_{Sol}(\lambda)} = \frac{3}{2}\left(\frac{Q_a(\lambda)}{a^*_{Sol}(\lambda)dc_i}\right),$$ (11)

where the ratio 3/2 is the geometrical factor for a sphere [see Morel, 1994]. Equations (9) and (10) are used to obtain $Q_a(\lambda)$ for calculating $Q^*_a(675)$ from $a^*_{Sol}(675)$ and dc_i (i.e., $\rho'(675)$). The computation can be greatly simplified, however. Solving the theoretical (11) for a range of $\rho'(675)$ normally found in phytoplankton (0.005 to around 6 [Agusti, 1991]), and fitting the results to an exponential function, $Q^*_a(675)$ can be described almost exactly ($n=1200$; $r^2=0.999$) with the function $Q^*_a(675) = m_1 + m_2 \exp(-m_3\rho'(675))$, where m_t are coefficients.

Because $a^*_{Sol}(675)$ is assumed constant in (11), the same functional form should describe the relationship between $a^*_{ph}(675)$ and dc_i. For a wide range of phytoplankton species grown in laboratory using diverse culturing methods (Figure 2a), the relationship is

$$a^*_{ph}(675) = 0.00767 + 0.0227e^{(-0.0376dc_i)}.$$ (12)

Thus (12) is an approximation to the theory. This same exponential form was applied to derive a purely empirical expression for $a^*_{ph}(675)$ as a function of C (Figure 2b), using a

compilation of our phytoplankton absorption data (i.e., particulate corrected for detrital absorption) and the data from Bricaud et al. [1995]:

$$a^*_{ph}(675) = 0.0110 + 0.0158e^{(-0.311C)}.$$ (13)

The relationship between dc_i and C was obtained by equating (12) and (13) and solving for dc_i (Figure 2c):

$$dc_i = -26.59\ln(0.147 + 0.696e^{(-0.311C)}).$$ (14)

The result, at a given C, is dc_i for an average cell that represents the entire phytoplankton community. It is important to stress that (14) is at best an approximation of the central tendency of both field and laboratory data sets used here. Thus, combining equations (9), (10), and (11), we obtain

$$a^*_{ph}(\lambda) = \frac{3}{2dc_i}\left(1 + \frac{2e^{-a^*_{Sol}(\lambda)dc_i}}{a^*_{Sol}(\lambda)dc_i} + \frac{2\left(e^{-a^*_{Sol}(\lambda)dc_i} - 1\right)}{(a^*_{Sol}(\lambda)dc_i)^2}\right).$$ (15)

Our goal in generating this approximation was to allow the parameterization of phytoplankton absorption with two terms: one dominated by packaging and one dominated by changes in accessory pigments so that different types of communities could be tested in our sensitivity analysis. Although the compiled data were extensive, the use of this equation is limited to the assumptions that we have made, the data set used, and to the models chosen for the curve fits. Error bars in Figure 2c represent two standard deviations, computed using the Delta method, an approximation to a Taylor series [Bishop et al., 1975]. In this method, the variance is computed as the product of a matrix containing the variance and covariance terms of each fit and a vector containing the first derivatives of the final expression (14) evaluated at each C with respect to each of the six fitted parameters.

3.1.1.2. Pigment composition. At wavelengths other than 675 nm, the absorption by accessory pigments cannot be neglected. The spectral dependence of a^*_{Sol} for the

---

Figure 1. Parameterization of $K_d(490)$ and $L_u(443)/L_u(550)$ as functions of C (see Notation section for symbols, and text for details). Absorption and backscatter, then attenuation and spectral reflectance, were predicted from C consistent with bio-optical relationships derived from theory (inverted triangle), laboratory studies (circle), and empirical relationships from the field (hexagons). Spectral absorption: Specific absorption coefficients, $a^*_{ph}(\lambda)$, were described as functions of C using exponential fits to data from surface waters. Pigment packaging (a function of cellular diameter and pigment concentration, dc_i) was estimated as a function of C by combining the relationship between $a^*_{ph}(675)$ and dc_i from laboratory with $a^*_{ph}(675)$ as a function of C from the field (at 675 nm, the influence of accessory pigments can be neglected). Given $a^*_{ph}(\lambda)$ and dc_i, the influence of accessory pigmentation (unpackaged absorption, $a^*_{Sol}(\lambda)$) on $a^*_{ph}(\lambda)$ as a function of C is described for seven wave bands by using iterative solutions for $a^*_{Sol}(\lambda)$, the one remaining unknown in the theoretical anomalous diffraction approximation [van de Hulst, 1957]. Absorption by CDOM + detritus at 443 nm, $a_{cdom+det}(443)$, is described as a linear function of phytoplankton absorption, $a_{ph}(443)$, with an intercept (D_0) and slope (d_s) consistent with field data; $a_{cdom+det}$ at other wavelengths is calculated with a spectral slope factor S. Absorption by water, $a_w(\lambda)$, comes from the literature. Spectral backscatter: Both scattering by phytoplankton plus detritus at 660 nm, $b_{ph+det}(660)$, and the backscatter ratio, $\tilde{b}_{b_{ph+det}}$ are specified as functions of C using published empirical relationships. Their product is used to calculate $b_{b_{ph+det}}(\lambda)$ with the application of an exponential slope (γ) for wavelength dependence. The slope changes with trophic status, reflecting larger particle sizes at higher C. Backscatter due to pure water, $b_{b_w}(\lambda)$, comes from the literature. To estimate $K_d(490)$, an average cosine $\bar{\mu}_d$ of 0.7 is assumed. To calculate the blue:green radiance ratio, $L_u(443)/L_u(550)$, a value for M of 0.95 is assumed to account for the influence of the light field. The model is novel in that it integrates well-known relationships between optical properties and C with other bio-optical relationships to achieve predictions of absorption and scatter as functions of C that by design are consistent with a large body of data from the field and laboratory. This general approach can be modified to calculate any properties that depend on absorption, scatter, or, as functions of C, backscatter.
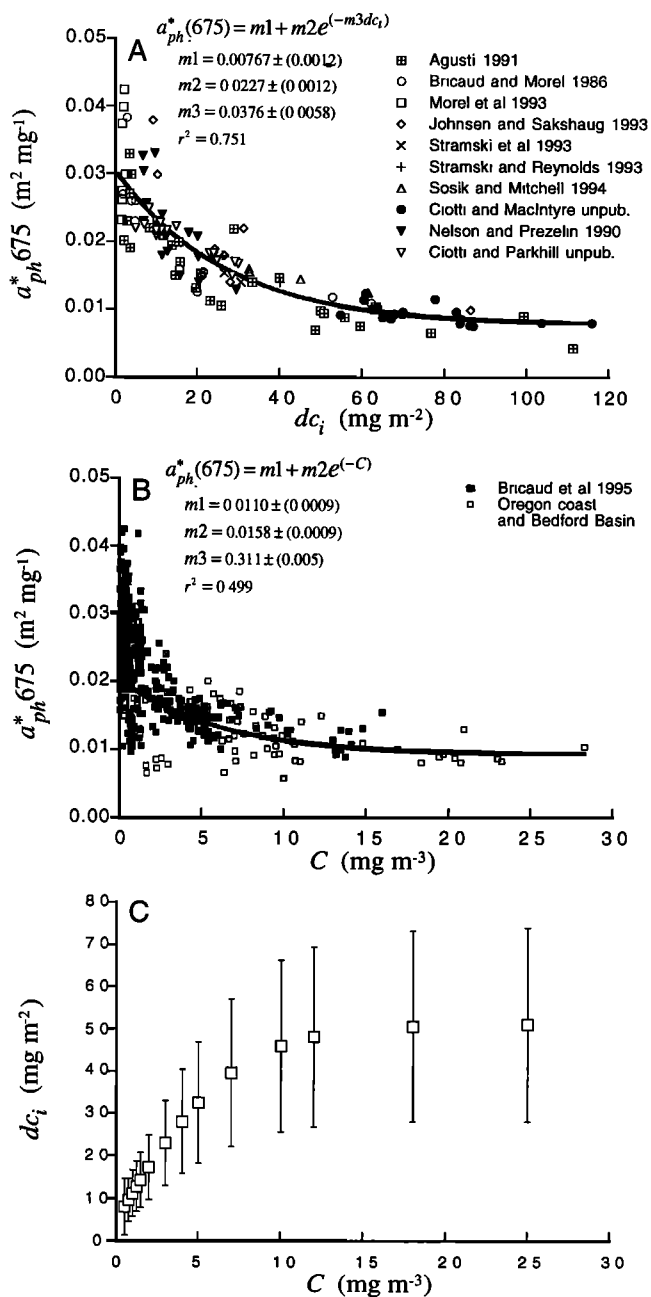
Figure 2. Steps for estimating the product of the cell diameter and the intracellular pigment concentration (dc_i) as a function of trophic status. (a) Empirical relationship between $a_{ph}^*(675)$ and the product of cell diameter (d) and the intracellular concentration of pigments (c_i) for data from cultures. See references for species, media, and light regime. A. M. Ciotti and J. G. MacIntyre (unpublished data, 1995) refers to the toxic dinoflagellate *Alexandrium tamarense* grown in K media in semicontinuous culture (see MacIntyre et al. [1997] for details), and A. M. Ciotti and J. P. Parkhill (unpublished data, 1997) refers to the coastal diatom *Thalassiosira pseudonana* in continuous culture. Table in the figure indicates equation form, parameter values, and respective standard deviations, and r^2. (b) Empirical relationship between $a_{ph}^*(675)$ and C. Table indicates equation form, parameter values, and respective standard deviations, and r^2. (c) Approximation for a relationship between the product dc_i and C. This approximation was constructed by equating the relationships derived in Figures 2a and 2b. Error bars indicate two standard deviations computed using the Delta method (see text).

main accessory pigments of phytoplankton, as well as for chlorophyll a, has been described [*Bidigare et al.*, 1990; *Hoepffner and Sathyendranath*, 1991; see *Johnsen et al.*, 1994]. However, the ratio of accessory pigments to chlorophyll a is expected to change with trophic status [*Claustre*, 1994], thus modifying $a_{sol}^*(\lambda)$. Briefly, as the trophic status changes from eutrophic to oligotrophic (i.e., as C decreases), the mass ratio of accessory pigments to chlorophyll a increases [*Claustre*, 1994; *Gieskes et al.*, 1988], and in turn $a_{sol}^*(\lambda)$ will increase in the blue-green portion of the spectrum.

Because we do not know a priori the form by which $a_{sol}^*(\lambda)$ changes as a function of C, we followed five steps to derive an approximation (see Figure 1):

1. Empirical relationships between $a_{ph}^*(\lambda)$ and C for seven wave bands were derived using compiled data from the field, with C ranging from 0.03 to 32 mg m^{-3} (Table 1). The data for each wave band were averaged to be consistent with the spectral response of the sea-viewing wide-field-of-view sensor (SeaWiFS) ocean color satellite and with our optical instruments, which were designed to match SeaWiFS [*Cullen et al.*, 1994].

2. For each of the seven wave bands $a_{ph}^*(\lambda)$ was computed at 17 values of C (from 0.5 to 50 mg m^{-3}) using the empirical relationships derived in step 1.

3. For the same 17 values of C, dc_i was calculated with (14).

4. For each wave band and value of C, dc_i was substituted into (15) and $a_{sol}^*(\lambda)$ was estimated iteratively by minimizing the difference between $a_{ph}^*(\lambda)$ from (15) and $a_{ph}^*(\lambda)$ from step 2.

5. The final relationships between $a_{sol}^*(\lambda)$ and C were generated by least squares techniques (Figure 3, see equation form, parameters, and r^2 in Table 2). These curves represent the "residual" variation of $a_{ph}^*(\lambda)$ versus C, after taking empirically determined changes in packaging into account. We stress once more that these equations are approximations valid only for the range of C used (i.e., 0.5 to 30 mg m^{-3}).

Table 1. Parameters and Correlation Coefficient (r^2) Values for the Empirical Relationships Generated From the Field Data Set of $a_{ph}^*(\lambda)$ and C

Parameter	Wavelength (nm)					
	412	443	490	510	555	670
m1	0.012	0.013	0.010	0.008	0.004	0.008
sd m1	0.002	0.003	0.002	0.002	0.001	0.001
m2	0.039	0.076	0.050	0.015	0.005	0.011
sd m2	0.004	0.004	0.003	0.002	0.001	0.001
m3	3.123	2.987	2.984	0.202	0.132	0.256
sd m3	0.555	0.033	0.377	0.067	0.041	0.045
m4	0.308	0.026	0.020	0.027	ns	ns
sd m4	0.003	0.004	0.003	0.002	na	na
m5	0.308	0.214	0.232	2.979	ns	ns
sd m5	0.122	0.080	0.081	0.478	na	na
r^2	0.745	0.824	0.810	0.749	0.260	0.446

Equation is $a_{ph}^*(\lambda) = m1 + m2e^{(-m3C)} + m4e^{(-m5C)}$. Phytoplankton absorption spectra were averaged, consistent with the spectral response of the SeaWiFS ocean color sensor (about 20-nm wave bands centered on the wavelength designated). The data are a compilation of spectra with 2-nm resolution [*Bricaud et al.*, 1995] and our phytoplankton absorption data (1-nm resolution) collected off the Oregon coast [*Ciotti et al.*, 1996] and in a coastal embayment (Bedford Basin, Nova Scotia, Canada). C is chlorophyll a plus pheopigment concentration. The parameter values: ns, not significant; na, not available; sd, standard deviations for each parameter.
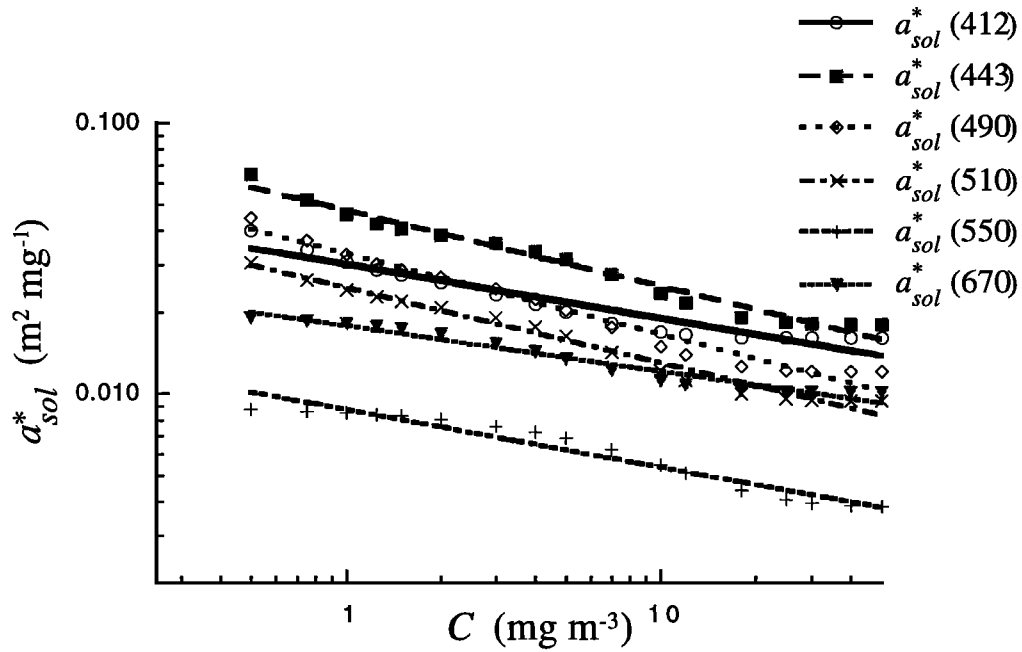
Figure 3. Best fit for derived values of $a^*_{sol}(\lambda)$ versus C at the SeaWiFS wave bands. See Table 2 for equation form, parameter values, and respective standard deviations, and r^2.

3.1.2. Parameterization of CDOM and detrital absorption.
Within the visible range (400 to 700 nm), CDOM absorption can be parameterized as

$$a_{cdom}(\lambda) = a_{cdom}(\lambda_0)e^{[S(\lambda-\lambda_0)]}, \quad (16)$$

where S (nm^{-1}) is the slope of the exponential decrease with wavelength and $a_{cdom}(\lambda_0)$ is the absorption coefficient for CDOM at one reference wavelength, usually between 400 and 440 nm [*Bricaud et al.*, 1981]. The slope S generally varies from -0.017 to -0.0115 nm^{-1} [*Carder et al.*, 1989] with a mean of -0.015 nm^{-1} for a variety of waters. Absorption by "detritus" follows the same spectral shape as CDOM absorption from 400 to 600 nm [*Bukata et al.*, 1983] with comparatively smaller slopes [*Roesler et al.*, 1989]. Because we are interested mainly in the blue and green regions, in our general model, absorption coefficients will be combined in a single term, $a_{cdom+det}(\lambda)$ [e.g., *Roesler and Perry*, 1995].

Different environments will have different sources of the detritus and CDOM (e.g., rivers versus autochthonous production), so a simple parameterization of $a_{cdom+det}(\lambda)$ with C is difficult. Nevertheless, an assumed linear relationship between detritus and phytoplankton absorption

Table 2. Parameters and r^2 Values for the Relationships Generated for $a^*_{sol}(\lambda)$ and C

Parameter	Wavelength (nm)					
	412	443	490	510	555	670
m1	0.0300	0.0460	0.0329	0.0245	0.0070	0.0178
sd m1	0.0007	0.0004	0.0005	0.0003	0.0001	0.0003
m2	0.2007	0.2525	0.2996	0.2781	0.0070	0.0178
sd m2	0.0149	0.0068	0.0115	0.0083	0.0069	0.0087
r^2	0.937	0.990	0.982	0.989	0.953	0.965

Equation is $a^*_{sol}(\lambda) = m1C^{-m2}$. This value was used in combination with equations (14) and (15) to solve for $a^*_{sol}(\lambda)$ for each C. The parameter values in the table describe the best fit for $a^*_{sol}(\lambda)$ and C. Standard deviations (sd) for each parameter are indicated.

can explain particular situations [see *Eppley et al.* 1977]. Although the linear relationships presented by *Eppley et al.*, [1977] were derived for phytoplankton and detrital carbon only, we will assume that the same type of relationship can be expected between phytoplankton absorption and a term combining detrital and CDOM absorption. The slope of this line represents the fraction that is directly associated or covaries with phytoplankton; the intercept represents a background value. Using 443 nm as a reference wavelength, $a_{cdom+det}(\lambda)$ is expressed as follows:

$$a_{cdom+det}(443) = D_0 + d_s a_{ph}(443), \quad (17)$$

where D_0 (m^{-1}) represents a background absorption that is not correlated with $a_{ph}(443)$, and d_s (dimensionless) is the slope of a linear relationship between $a_{ph}(443)$ and $a_{cdom+det}(443)$. This type of relationship was observed in our data collected off the Oregon coast; however, it may not hold in environments in which CDOM and/or detrital inputs and pools are highly variable. Once $a_{cdom+det}(443)$ is computed, the other wavelengths are estimated with (16) by assuming a value for S.

3.2. Total backscattering

Because backscattering by CDOM can be neglected [*Mobley*, 1994], the total backscattering coefficient can be partitioned into three components:

$$b_b(\lambda) = b_{b_w}(\lambda) + b_{b_{det}}(\lambda) + b_{b_{ph}}(\lambda). \quad (18)$$

Backscattering by seawater is assumed to be constant and the particulate components ($b_{b_i}(\lambda)$, m^{-1}) can be parameterized as follows [*Gordon et al.*, 1988; *Sathyendranath and Platt*, 1988]:

$$b_{b_i}(\lambda) = \tilde{b}_{b_i} b_i(\lambda), \quad (19)$$

where $b_i(\lambda)$ is the scattering coefficient by each component (i) and $\tilde{b}_{b_i}$ (dimensionless) is the correspondent

backscattering ratio, which is a function of the particle size and the real and imaginary parts of the refractive index [*Morel and Bricaud*, 1986].

The contribution of phytoplankton to the total backscattering coefficient is very small [*Stramski and Kiefer*, 1991, and references therein] because phytoplankton are generally large compared to the visible wavelengths and their refractive index is similar to that of seawater. Their backscattering ratios ($\tilde{b}_{b_{ph+det}}$) vary from around 0.0001 to 0.004 [*Morel and Bricaud*, 1981]. The source of most of the backscattering in the ocean is unknown and has been attributed to submicron inorganic particles and heterotrophic bacteria [*Morel and Ahn*, 1991; *Stramski and Kiefer*, 1991; *Ulloa et al.*, 1994] and more recently to bubbles [*Stramski*, 1994; *Zhang et al.*, 1998]. Because of that, empirical relationships between backscattering and C account for backscattering of the whole particle assemblage (which in our terminology would be $b_{b_{ph+det}}(\lambda)$) [*Gordon et al.*, 1988; *Gordon and Morel*, 1983; *Morel*, 1988; *Ulloa et al.*, 1994]. Thus

$$b_b(\lambda) = b_{b_w}(\lambda) + \tilde{b}_{b_{ph+det}} b_{ph+det}(\lambda) \qquad (20)$$

We will present the parameterization of scattering and backscattering ratio by particles, accounting for the influence of particle assemblages on the backscattering coefficient, and the spectral shape of backscatter. We stress that all these relationships with C are purely empirical and, because of the low contribution of phytoplankton to the bulk backscattering, they likely reflect the relationship of backscattering to factors that covary with phytoplankton changes, rather than the direct influence of phytoplankton.

3.2.1. Scattering by particles.
Empirical relationships between $b_{b_{ph+det}}(\lambda)$ and C are derived from measurements made predominantly in blue waters at a single wavelength, using data from transmissometers (i.e., at 660 nm) after correction for absorption by water. The most widely used relationship is the one proposed by *Morel* [1988], recently revisited by *Loisel and Morel* [1998]. The new analyses were partitioned into upper (mixed) and deep layers, and new data were included, expanding the range of C previously published. The mixed layer equation presented by *Loisel and Morel* [1998] showed a good agreement with our transmissometer data (after correcting for water and particulate absorption at 660 nm) and with chlorophyll data collected during the Oregon cruise and during a spring bloom experiment in Bedford Basin in 1993; thus it will be used to parameterize $b_{ph+det}(660)$:

$$b_{ph+det}(660) = 0.347 C^{0.766}. \qquad (21)$$

3.2.2. Backscattering ratio.
Existing relationships for $\tilde{b}_{b_{ph+det}}$ as a function of C [*Gordon et al.*, 1988; *Morel*, 1988] were established from estimated values which accounted for the expected decrease in $\tilde{b}_{b_{ph+det}}$ as C increases, due to the increasing contribution of larger particles with low backscattering efficiency [*Morel and Bricaud*, 1981]. Implicit in the selection of a particular $\tilde{b}_{b_{ph+det}}$, however, is an assumed size distribution for the whole particle assemblage. *Ulloa et al.* [1994], using Mie computations, showed that if the size distribution of particles with the same refractive index is modeled as a power law (or a Junge-type distribution), $\tilde{b}_{b_{ph+det}}$ is independent of wavelength, and its magnitude depends strongly on the exponent which describes the slope of the size

distribution: waters with a more negative exponent (i.e., smaller sizes are more important) will have a higher $\tilde{b}_{b_{ph+det}}$. Using inverse modeling of observed reflectance spectra, they derived an expression of $\tilde{b}_{b_{ph+det}}$ versus C consistent with empirical relationships presented by *Gordon et al.*, [1988] and *Morel* [1988]. Thus we will assume that $\tilde{b}_{b_{ph+det}}$ is independent of wavelength and dependent on C following *Gordon et al.*, [1988]:

$$\tilde{b}_{b_{ph+det}} = 0.013481 - 0.00651 \, \log10 \, (C). \qquad (22)$$

3.2.3. Wavelength dependence of backscattering.
Given that $\tilde{b}_{b_{ph+det}}$ is assumed to be wavelength independent, the spectral shape of particle backscattering will follow that of the particle scattering coefficient. *Aiken et al.* [1992] assumed that the wavelength dependence of $b_{b_{ph+det}}(\lambda)$ was approximately λ^{-1}. It has been shown, however, that from oligotrophic to eutrophic waters, the spectral dependence of particle scattering changes. In oligotrophic waters, the total scattering coefficient has been shown to follow both λ^{-2} [*Sathyendranath et al.*, 1989] and λ^{-1} [*Mobley*, 1994; *Morel*, 1988], consistent with the dominance of small particles. In eutrophic environments, the total scattering has been shown not to vary much with wavelength [*Gordon et al.*, 1988; *Morel*, 1988], related to the addition of bigger particles with flatter scattering spectra. To account for this change with trophic status, we will assume that the scattering coefficient follows λ^{-2} when C is low (0.05 mg m^{-3}) and λ^0 when C is high (20 mg m^{-3}) [*Gordon et al.*, 1988] and that the exponent decreases logarithmically with C. Accordingly,

$$b_b(\lambda) = b_{b_w}(\lambda) + \tilde{b}_{b_{ph+det}} b_{ph+det}(660)\left(\frac{660}{\lambda}\right)^{\gamma}, \qquad (23)$$

where γ decreases from 2 to 0 following a logarithmic function of C:

$$\gamma = 1 - 0.768 \, \log10 \, (C). \qquad (24)$$

4. Implementation of the Semi-analytical Model

We can now calculate both $K_d(490)$ and $L_u(443)/L_u(550)$ as functions of trophic status. The approach is shown in Figure 1, and the equations are given in section 3. $K_d(490)$ is given by

$$K_d(490)_k = \frac{a_{ph}(490)_k + e^{(-47S)}(D_o + d_s a_{ph}(443)_k) + a_w(490)}{\overline{\mu}_d}, \qquad (25)$$

and $L_u(443)/L_u(550)$ is given by

$$\left(\frac{L_u(443)}{L_u(550)}\right)_k = 0.95 \left[\frac{(b_{b_w}(443) + b_{b_{ph+det}}(660)_k 1.49^{\gamma_k})}{(b_{b_w}(550) + b_{b_{ph+det}}(660)_k 1.2^{\gamma_k})} \times \right.$$
$$\left. \frac{a_{ph}(550)_k + e^{(-107S)}(D_o + d_s a_{ph}(443)_k) + a_w(550)}{D_o + a_{ph}(443)_k(1 + d_s) + a_w(443)}\right], \qquad (26)$$

where γ designates the spectral dependence of the particle scattering and k represents the evaluation of each term for a given C value. In these equations

$\bar{\mu}_d=0.7$ (see section 2.2);

$S=-0.015$ (nm^{-1}, see section 3.1.2);

$D_0=0.02$ (m^{-1}, simulating an oligotrophic $a_{cdom+det}$ background [Kirk, 1994b]),

$d_s=0.3$ (following Bricaud and Stramski [1990]).

Assuming that this general model has the same form as empirically derived relationships [Aarup et al., 1996; Austin and Petzold, 1981; Mueller and Trees, 1997],

$$\ln(K_d(490) - K_{d_w}(490)) = A_0 + A_1 \ln(L_u(443)/L_u(550)), \quad (27)$$

where $K_{d_w}(490)$ is the attenuation coefficient of pure water at 490 nm. The parameters A_0 and A_1 can be estimated statistically for predictive purposes given solutions of (25) and (26) over a range of C. For different environments and/or different assumptions, the parameters and relationships with C are expected to differ, as we will show later. Nevertheless, the basic principles will hold and new relationships can be derived accordingly. Hereinafter, this general model will be referred to as the Semi-analytical Model of Ocean Color and Attenuation as a Function of Trophic Status (SAMOCAFOTS). The model predicts absorption and backscatter in the ocean, and hence attenuation and spectral reflectance, as a function of surface chlorophyll, consistent with well-described bio-optical relationships derived from theory, laboratory research, and measurements in the field. Therefore it reconciles a broad range of known relationships between phytoplankton community structure, optical properties of surface waters, and trophic status of surface waters.

It is acknowledged that modeling optical properties as functions of chlorophyll concentration can introduce many limitations, mainly regarding the imprecise relationship between chlorophyll and phytoplankton biomass [Cullen, 1982]. Nonetheless, chlorophyll is the single most evident descriptor of phytoplankton abundance, and understanding how different communities influence optical properties is an important starting point to a better interpretation of bio-optical models. The results of our sensitivity analysis (see below) reveal how different communities influence optical properties at a given chlorophyll concentration.

The validation of the semi-analytical model is done through comparisons with empirical relationships between diffuse attenuation at 490 nm, $K_d(490)$, and ratios of upwelling radiance of 443 to 550 nm, $L_u(443)/L_u(550)$. These particular wavelengths were selected due to the availability of several empirical relationships [e.g., Aarup et al., 1996; Austin and Petzold, 1981; Mueller and Trees, 1997] and a large independent data set. By adjusting a few parameters (see below), the model can easily include other wavelengths.

5. Bio-optical Field Data

Bio-optical data at the surface were collected during a number of cruises (Table 3). For sampling details during the Bedford Basin summer experiments (BBS92 and 93) and the cruise off Oregon (ORE94), refer to Cullen et al. [1994] and Ciotti et al. [1996], respectively. Chlorophyll (fluorometric) as well as particulate (filter pad method) and dissolved absorption were measured as described by Ciotti et al. [1996]. Data from the 1996 time series in Bedford Basin (BBTS96) were collected every 10 min with a tethered attenuation coefficient chain sensor, which was moored in Bedford Basin

Table 3. List of Cruises With Respective Location, Dates and Optical Measurements at the Surface

Cruise	Location	Dates	Optical properties measured near-surface
ORE94	off the Oregon coast	September 1994	$L_u(443)$, $L_u(555)$, $K_d(490)$
WE97	Bering Sea	April 1997	$L_u(443)$, $L_u(555)$, $K_d(490)$
BBS92	Bedford Basin	August 1992	$L_u(443)$, $L_u(555)$, $K_d(490)$
BBS93	Bedford Basin during a red tide	August 1993	$L_u(443)$, $L_u(555)$, $K_d(490)$
BBTS96	Bedford Basin	June to November 1996	$L_u(443)$, $L_u(559)$, $K_d(490)$

from July to November. This instrument is a radiometer buoy measuring spectral upwelling radiance ($L_u(\lambda)$) in seven wave bands at a depth of 0.45 m, and a chain containing four $E_d(490)$ sensors, positioned at 2, 4, 8, and 16 m, with another 30 cm above the surface. Surface (upper 2 m) $K_d(490)$ was computed using estimated $E_d(490)$ just below the surface (i.e., $E_d(490)$ in the air corrected for Fresnel reflectance [see Mobley, 1994], assuming wind speed equal to zero) and the $E_d(490)$ sensor from 2 m. Because $L_u(\lambda)$ sensors are located at a depth of 0.45 m, $L_u(443)$ and $L_u(550)$ were propagated to just below the surface using the empirically determined spectral model of Austin and Petzold [1986] for $K_d(\lambda)$ as a function of $K_d(490)$. Independent $K_d(\lambda)$ data were obtained throughout the experiment confirming the appropriateness of this model for Bedford Basin during the study period.
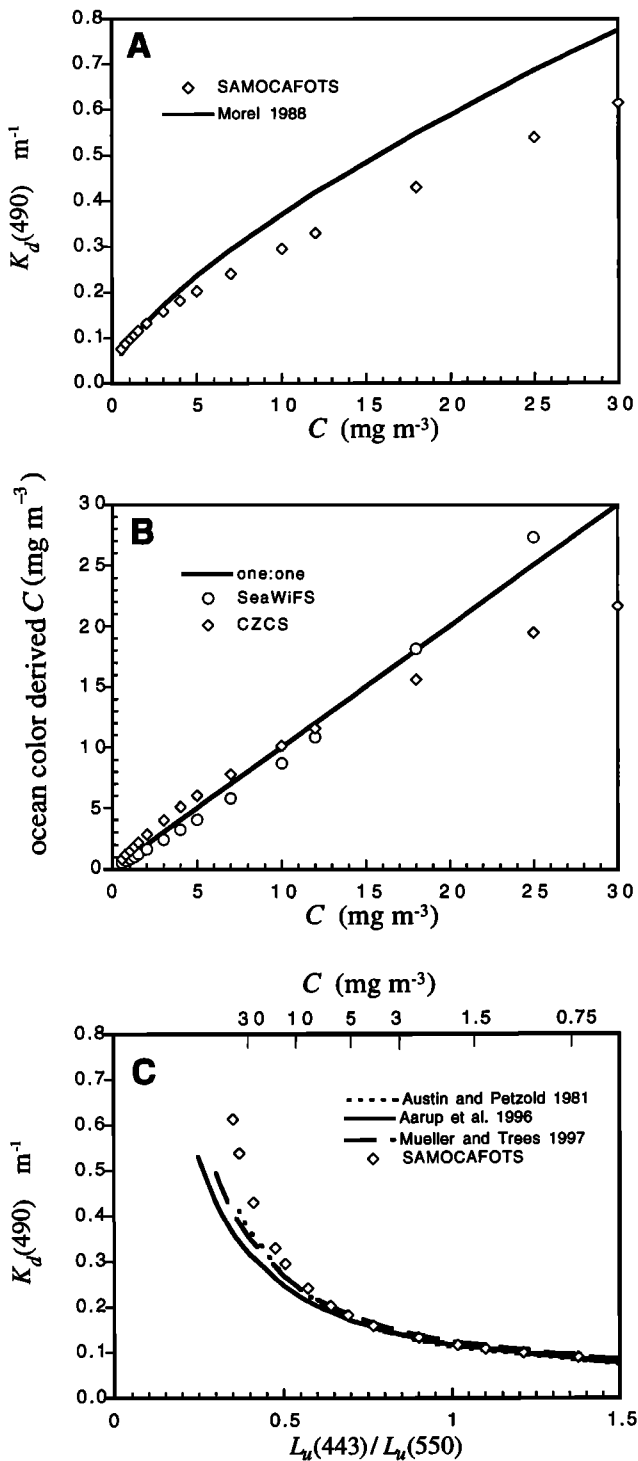
During the WE97 cruise (Table 3), a radiometer buoy measuring radiance reflectance ($L_u(\lambda)$ and $E_d(\lambda)$ in 13 wave bands) and a profiling radiometer measuring $E_d(\lambda)$ in the same wave bands were used. Sampling design and data processing were similar to those used during the ORE94 cruise, but because the radiance sensors were very close to the surface, $L_u(\lambda)$ was not corrected for attenuation.

6. Results and Discussion

6.1. Model Versus Established Empirical Relationships

We now compare our parameterization of $K_d(490)$ and $L_u(490)/L_u(550)$ with established empirical relationships.

6.1.1. Diffuse attenuation versus C. For $K_d(490)$ as a function of C, we used the relationship described by Morel [1988] (Figure 4a). Our parameterization of $K_d(490)$, which is based on data from laboratory and field, agreed to within 20% of the empirical relationship based on direct measurements, varying from overestimating by 20% at 0.5 mg m^{-3} to underestimating by 15% at 10 mg m^{-3}; above 10 mg m^{-3}, our model values remained 15% less than the empirical relationship. These results suggest some small inconsistencies in the parameterization of absorption by phytoplankton and/or by detritus plus CDOM. Although the visual comparison of model and empirical data in Figure 4a makes it tempting to infer that our parameterization underestimates total absorption (see (6)), the disagreement could also be a result of the form of the equation chosen to
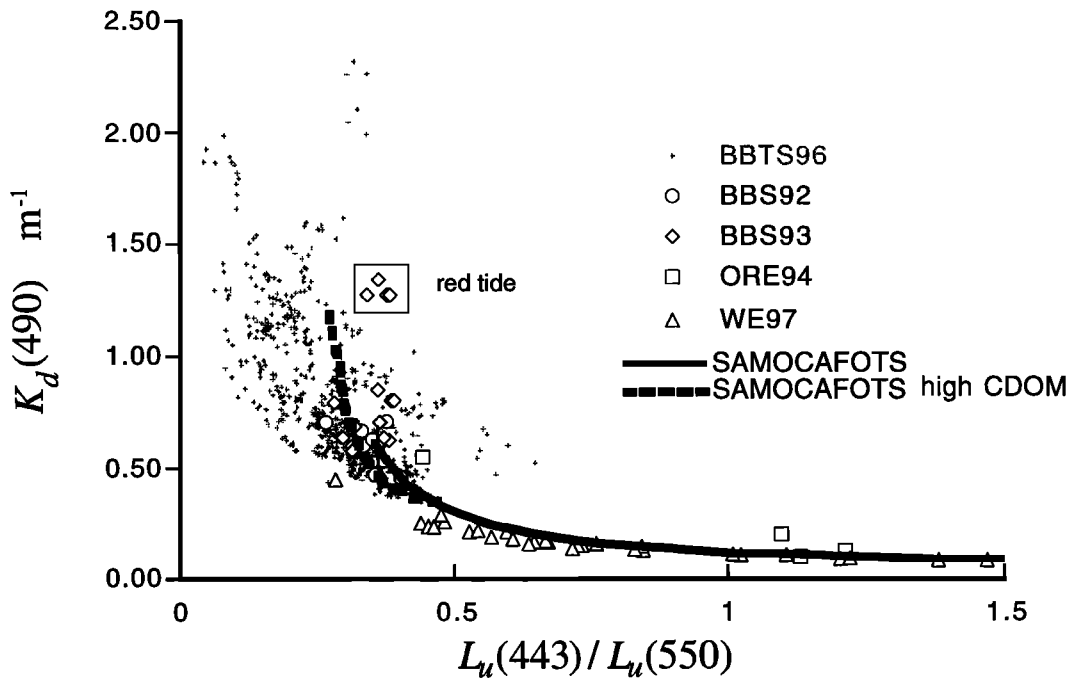
represent the field data, and also from keeping a constant value for the average cosine (see section 2.2). Nonetheless, considering all the assumptions that we made and the variability in the field data, the agreement is good: our semi-analytical expressions for IOPs, derived from basic bio-optical principles and relationships, reproduced well a statistically derived relationship between AOPs.

6.1.2. Retrieval of C from ocean color. The comparison between our parameterization of reflectance ratios and empirical data was done for relationships between C and $L_u(490)/L_u(550)$, computed as in (26) and modifying relevant parameters from 443 to 490 nm. In coastal waters, 490 nm has been shown to work better than 443 nm [e.g., Aiken et al., 1995, and references therein], and the new global algorithms for retrieving C from ocean color are now based on $L_u(490)/L_u(550)$. For a range of C, we used our model to compute $L_u(490)/L_u(550)$, which could be related to remotely sensed C (RSC) using published algorithms (Figure 4b). Two empirical RSC models were used: the coastal zone color scanner (CZCS) algorithm for RSC >1 mg m^{-3} (see Lewis and Cullen [1991], but note that the original algorithm was established for 500 to 560 nm) and the more recent SeaWiFS algorithm [O'Reilly et al., 1998]. Both empirical algorithms were derived with a very limited number of data points at high C, so comparisons at high C are meaningless. This analysis (Figure 4b) resulted in a good agreement (within 20%) between C used to compute $L_u(490)/L_u(550)$ and the retrieved RSC (inversion of $L_u(490)/L_u(550)$) using the SeaWiFS algorithm for C from 0.5 to 30 mg m^{-3}. Using the CZCS algorithm to retrieve RSC, the agreement was lower overall, and the retrieved C agreed within 20% with input C from 5 to 18 mg m^{-3}. These comparisons also demonstrate how our semi-analytical expressions for IOPs derived from basic bio-optical principles can reconcile relationships between AOPs and C.

6.1.3. Diffuse attenuation versus radiance ratio. Empirical models relating $K_d(490)$ to $L_u(443)/L_u(550)$ [Aarup et al., 1996; Austin and Petzold, 1981; Mueller and Trees, 1997] and the results derived by SAMOCAFOTS are shown in Figure 4c. The agreement between our model and the empirical relationships, and the agreement among the empirical relationships, is good for C up to 10 mg m^{-3}. Divergence among the different empirical models is noticeable in green waters ($L_u(443)/L_u(550) <$ 0.5), reflecting the bio-optical differences among data sets, differences in sample size, and the ranges of $K_d(490)$ and $L_u(443)/L_u(550)$ included in each. SAMOCAFOTS also diverges from the empirical relationships when $L_u(443)/L_u(550) <$ 0.5, that is, $C >$ 12 mg m^{-3} with more influence of CDOM (see below). However, the fact that a good agreement was possible without adjusting any of the parameters suggests that the simplifications and assumptions made in deriving the semi-analytical model are valid at least for C between 0.5 and about 15 mg m^{-3}.

6.2. Model Versus Independent Bio-optical Data

We now compare the semi-analytical model with independent optical measurements of $L_u(443)/L_u(550)$ and $K_d(490)$ (Figure 5). For $L_u(443)/L_u(550)$ from 0.5 to about 1.5, the general model explained most (above 90%) of the variability in $K_d(490)$ found in the field data. Note that the data from the Bering Sea cruise in 1997 tended to remain below the line defined by the general model. For radiance ratios

Figure 4. Comparison between empirical models and the parameterization of SAMOCAFOTS. (a) Attenuation coefficient at 490 nm versus the empirical model by Morel [1988]. (b) Radiance ratio of 490 to 550 nm ($L_u(490)/L_u(550)$) which was calculated as in (26) with the relevant parameters modified from 443 to 490 nm (see text). Comparison with the CZCS algorithm for $C >$1 mg m^{-3} [see Lewis and Cullen, 1991] and the more recent SeaWiFS algorithm [O'Reilly et al., 1998]. (c) SAMOCAFOTS and empirical models relating $K_d(490)$ to $L_u(443)/L_u(550)$ derived by Austin and Petzold [1981], Aarup et al. [1996], and Mueller and Trees [1997]. Note that empirical models were not extrapolated beyond the upper limit of $K_d(490)$ measured in each case.

Figure 5. Comparison of SAMOCAFOTS with independent data collected in a variety of coastal waters: off the Oregon coast in September 1994 (ORE94 [see *Ciotti et al.*, 1996]), in the Bering Sea in June of 1997 (WE97), and in Bedford Basin on several occasions: summer of 1992 (BBS92), summer of 1993 (BBS93) during a red tide event (in box [*Cullen et al.*, 1994]), and also a time series from June to November of 1996 (BBTS96). Plot shows data from BBTS96 collected daily between 11:00 and 13:00 local time. Note that the radiance ratios measured during ORE94, BBS92, and BBS93 were between 443 and 555 nm and during BBTS96 were between 443 and 559 nm.

below 0.5, however, it is clear that no single relationship can explain the dispersion of the data, especially those derived from Bedford Basin. These data suggest that a family of curves can be derived and show also a group of outliers associated with a red tide event during BBS93 [*Cullen et al.*, 1994].
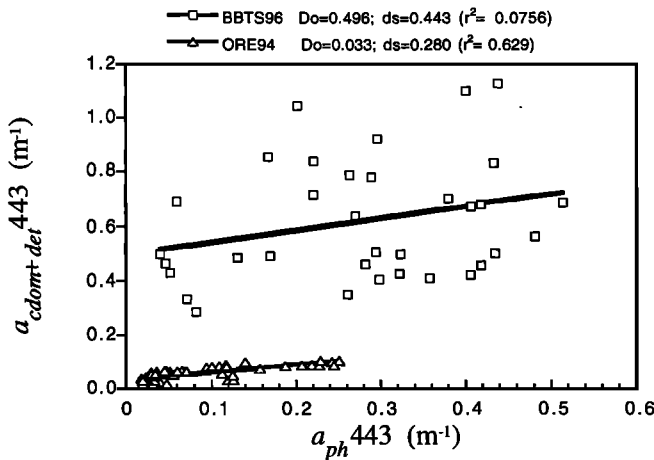
Figure 6. Absorption by detritus (particulate material after extraction with an organic solvent) plus CDOM and phytoplankton absorption at 443 nm during the weekly sampling in Bedford Basin in 1996 (BBST96) and during the Oregon cruise in September 1994 (ORE94). Lines represent an assumed linear relationship: the slope represents the fraction that is directly associated with phytoplankton and covaries with them (d_s) and the intercept represents a background value (D_0).

The most obvious differences among the data collected in Bedford Basin and the other data sets are related to the higher influence of CDOM and detritus in Bedford Basin. From absorption data collected weekly in Bedford Basin in 1996 (Figure 6; data from the Oregon cruise is plotted for comparison) we observed that the parameters describing CDOM plus detrital absorption (D_0 and d_s) differed from the original parameterization, although the slope S was in average close to -0.015. Thus to encompass more properly the range of conditions in Bedford Basin a second curve was constructed by using the same parameter values as in SAMOCAFOTS, except that D_0 and d_s were set to 0.4 m^{-1} and 0.4, respectively. The C range was also extended to 50 mg m^{-3}. Hereafter this relationship will be referred to as SAMOCAFOTS high CDOM.

Although SAMOCAFOTS high CDOM can explain some of the variability of the high $K_d(490)$ data as a function of C, the sources of the residuals about this mean relationship remain to be examined. In what follows, we developed an analysis to examine the independent influences of (1) packaging (dc_i) and pigment composition ($a^*_{sol}(\lambda)$), (2) the dependence of the scattering coefficient on wavelength (γ), and (3) the effects of CDOM and detrital absorption ($a_{cdom+det}(\lambda)$).

6.3. Sensitivity Analysis

We constructed relationships between $K_d(490)$ and $L_u(443)/L_u(550)$ using a range of fixed values for individual input parameters that were functions of C in SAMOCAFOTS (see Table 4). As mentioned above, the goals of this analysis

Table 4. Values for the Parameters and Variables Used in the Sensitivity Analysis

Input variables	Values
C, mg m^{-3}	0.5, 0.75, 1, 1.25, 1.5, 2, 3, 4, 5, 7, 10, 12, 18, 25, and 30 plus 40 and 50 for SAMOCAFOTS high CDOM
$a^*_{sol}(\lambda)$, m^{2}mgChl^{-1}	Corresponding to equations in Table 2
dc_i, mg m^{-2}	10, 20, 40, 60, 80, 100, and 120
γ	2, 1, 0, and -0.5
D_o, m^{-1}	0.0, 0.03, 0.06, 0.1, 0.2, 0.3, and 0.5
d_s	0.0, 0.1, 0.3, 0.5, and 0.8
S, nm^{-1}	-0.010, -0.012, -0.016, -0.018, -0.020, and -0.025

These values replaced the relationships with C in the general model. The parameter γ refers to the exponent of the relationship between particle scattering and wavelength.

were to identify the sources of the residual variability and to identify the effect of changes in phytoplankton community structure on this relationship.

6.3.1. Packaging and Pigment Composition. The idealized parameterization of phytoplankton absorption in our model accounted for changes in community structure as C increased, which was consistent with empirical relationships between $a^*_{ph}(\lambda)$ and C. Packaging and pigment composition were treated separately so that we could analyze the effects of different cell sizes with distinct pigment composition.

In order to simulate the effects of pigment packaging, we reconstructed the curves of $K_d(490)$ versus $L_u(443)/L_u(550)$ using the SAMOCAFOTS parameterizations but substituting constant dc_i for all C values (Table 4). The influence of different pigment composition was analyzed in a similar manner: the terms of $a^*_{sol}(\lambda)$ which varied with C (Table 2) were replaced with fixed values. Because three wavelengths are involved, we computed $a^*_{sol}(443)$, $a^*_{sol}(490)$, and $a^*_{sol}(550)$ for three concentrations of C (1, 5, and 20 mg m^{-3}), representing high, middle and low accessory pigmentation, respectively [*Claustre*, 1994]. The goal was to keep the proportions among the three wavelengths consistent with field observations.

Both packaging and pigment composition strongly affected the shapes of the curves (Figure 7). Some of the combinations of parameter values resulted in reconstructed curves that were close to the general models (and consequently, close to the empirical models). However, no single combination was able to reproduce these models completely for the given ranges of C. The general trend in the model was in accordance with expected changes in phytoplankton composition as C increases can be seen in Figure 7: as cell size, hence dc_i, increases [*Chisholm et al.*, 1988; *Malone*, 1980; *Yentsch and Phinney*, 1989], the ratio (mass to mass) of accessory pigments to chlorophyll a decreases [*Claustre*, 1994], thus decreasing $a^*_{sol}(\lambda)$. The combinations of fixed parameters created an "envelope" around the general relationship. Not surprisingly, the most significant deviations were observed when phytoplankton communities were composed of cells that were "opposed" to the normal trend, that is, small and less pigmented cells dominating at high C, or bigger cells that were heavily pigmented. These are possible occurrences in

coastal and estuarine waters. For example, blooms of *Skeletonema costatum* have low dc_i [see *Morel and Bricaud*, 1986] and blooms of some dinoflagellates (e.g., *Alexandrium tamarense* in laboratory experiments) show high dc_i values from 55 to 116 mg m^{-2}.

Deviations occur in both $K_d(490)$ and $L_u(443)/L_u(550)$ as functions of C (see examples for "medium" accessory pigments in Figure 8). For a given C, bigger cells show higher reflectance ratios and smaller attenuation than the general tendency (SAMOCAFOTS). The two effects combined make the relationship between $K_d(490)$ and $L_u(443)/L_u(550)$ deviate to the upper part of the "envelope" observed around the expected central tendency. Conversely, dominance of small and "pale" cells push the relationship to the lower part of the envelope. The same trends were observed in the sensitivity analysis using SAMOCAFOTS high CDOM (Figures 7d, 7e, and 7f).

Some of the deviations observed in our data set (Figure 5) can indeed be related to the "size" of the dominant organism. During the red tide event (BBS93), when large dinoflagellates (*Gonyaulax digitale* and *Dinophysis spp.*) were at depth and the surface community was composed of small flagellates, the observations approached the general relationships. When the dinoflagellate cells were at the surface, the observations clearly deviated to the upper portion of the "envelope" [*Cullen et al.*, 1994]. During the cruise in the Bering Sea in 1997, observations clustered to the lower portion at high C. These samples were dominated by colonies of *Phaeocystis sp.* (J. J. Cullen et al., unpublished data, 1997) containing small cells.

Thus, as a first approximation, deviations from the general relationship between $K_d(490)$ and $L_u(443)/L_u(550)$ could be used as a way to detect and characterize blooms optically. This might only work at a regional level, because the establishment of a precise general relationships relies on knowledge of how the several parameters covary with C (equations (25) and (26)).

6.3.2. Spectral dependence of total scattering. As discussed in section 3.2, the particle backscattering coefficient can generally be represented by an inverse-wavelength dependent spectrum [see *Mobley*, 1994]. In SAMOCAFOTS, its exponent (γ) followed an assumed logarithmic relationship with C, going from λ^{-2} at low C grading to λ^0 at high C, representing the importance of small and large particles, respectively. The sensitivity of SAMOCAFOTS to γ was thus established by substituting its relationship with C with fixed values from -2 to 0.5 (Figure 9). The effect of changes in γ appears small for the more commonly reported exponents of -1 to 0, becoming increasingly important as C increases (Figure 9a). The effect is larger when the absorption by CDOM plus detritus is important (Figure 9b).

The apparent change of the exponent from -2 or -1 to 0 is a "mean" observation [*Gordon et al.*, 1988; *Morel*, 1988; *Sathyendranath et al.*, 1989]. Comparison of SAMOCAFOTS with the *Austin and Petzold* [1981] empirical relationship at high $K_d(490)$ (Figure 9a) suggests that the exponent could exceed 0 in eutrophic waters. Further investigation of the relationships between particle backscattering and C in these waters is required, especially given that laboratory experiments with large phytoplankton species have shown spectral features of b_b that do not necessarily conform to a simple relationship with wavelength [*Stramski and Kiefer*, 1991]. This will be probably the case when blooms occur,
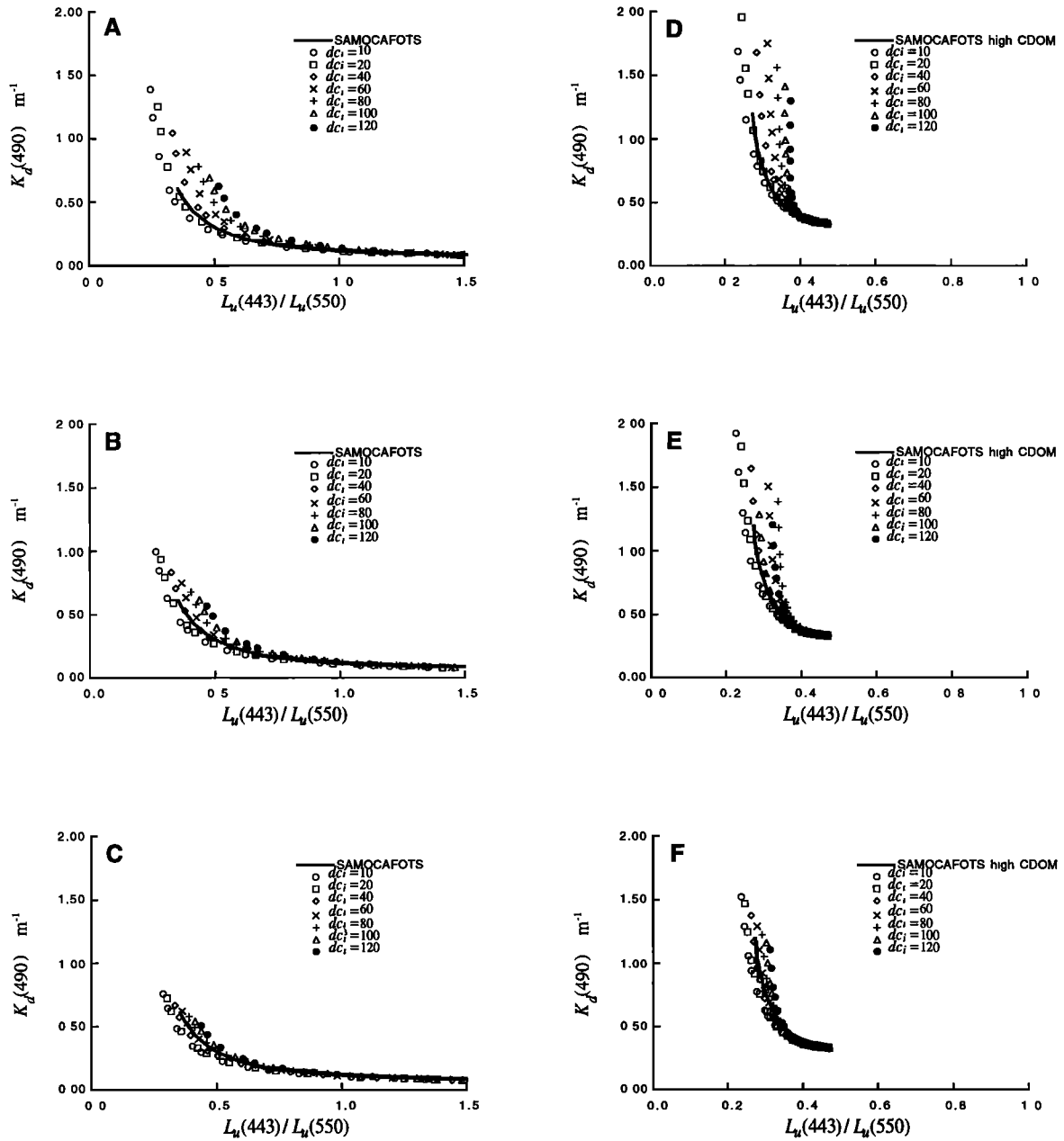
Figure 7. Results of the sensitivity analysis of the effects of changes in packaging and pigment composition. Individual points represent fixed values of the product of cell diameter and intracellular concentration of pigments, dc_i (see legend). Three fixed levels of $a^*_{sol}(\lambda)$ were used to represent high to low influence of accessory pigments, following the equations in Table 2 for C concentrations of (a and d) 1 mg m^{-3}, (b and e) 5 mg m^{-3}, and (c and f) 20 mg m^{-3}. All the other parameters are a function of C, as in SAMOCAFOTS and SAMOCAFOTS high CDOM, respectively.

because one particular group dominates the optical properties [e.g., Subramaniam and Carpenter, 1994]. If a bloom of bigger cells (high packaging) had a large influence on the total scattering coefficient or on the backscattering ratio [Ahn et al., 1992], it would result in positive exponents. In this case, the effect could counteract the effect of packaging on the deviations in the relationship between $K_d(490)$ and $L_u(443)/L_u(550)$. Thus it will be probably necessary to measure directly both absorption and scattering signatures for pertinent groups of phytoplankton in the field during blooms.

This analysis also suggests that input of different sizes of inorganic and organic material can strongly affect the

relationship between $K_d(490)$ and $L_u(443)/L_u(550)$. The inclusion of such particles, in addition to particle assemblage parameterized in SAMOCAFOTS can be easily done by the addition of an extra term in (23), such that

$$b_b(\lambda) = b_{bw}(\lambda) + \tilde{b}_{b_{ph+det}} b_{ph+det}(660)\left(\frac{660}{\lambda}\right)^\gamma$$

$$+ \tilde{b}_{b_{non-ph}} b_{non-ph}(660)\left(\frac{660}{\lambda}\right)^{\gamma_{non-ph}}, \qquad (28)$$

where $\tilde{b}_{b_{non-ph}}$ is the backscattering ratio for the additional particles and $b_{non-ph}(660)$ is its respective scattering
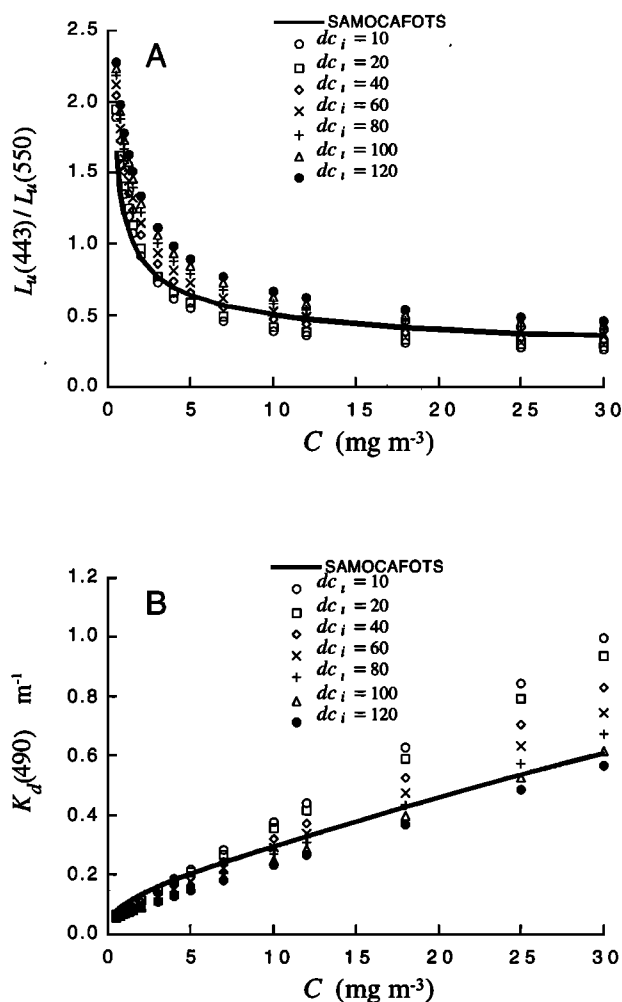
Figure 8. Analysis of the effects of changes in packaging for a fixed pigment composition ("medium" accessory pigments, as in Figure 7b) and the relationships between: (a) $L_u(443)/L_u(550)$ and C, and (b) $K_d(490)$ and C. Individual points refer to fixed values of the product of cell diameter and intracellular concentration of pigments, dc_i (legend) and $a^*_{sol}(\lambda)$ computed as in the equations in Table 2 for C equal to 5 mg m^{-3} ("medium" accessory pigments). Symbols indicate dc_i values in both graphs. Solid line is our model.

coefficient at 660 nm. As was done for phytoplankton plus detritus, once $bb_{non-ph}(660)$ is estimated, a spectral dependency (γ_{non-ph}) has to be assumed. Particles such as clay can have a backscattering ratio of up to 0.08 [*Bukata et al.*, 1983], and if a dependency of λ^{-1} is assumed, significant deviations from the general trend can result from increasingly larger inputs of these particles (Figures 10a and 10b). The input of these additional particles in Figures 10a and 10b is simulated by increasing the value of their scattering coefficient, $b_{non-ph}(660)$.

On the other hand, the input of particles with low backscattering ratios, small slopes, and no spectral dependency for the scattering coefficient (for example, organic particles with backscattering ratio 0.01), influence the relationship only slightly (Figures 10c and 10d), especially in situations where the proportion of $a_{cdom+det}$ to a_{ph} is high. Nevertheless, a large input of organic particles (for example, in Bedford Basin) with absorption spectra that

differ from those of the oceanic phytoplankton and detritus will affect the relationship between total absorption and C, as described below.

6.3.3. CDOM and detrital absorption. The effects of $a_{cdom+det}(\lambda)$ can be analyzed by varying: D_0, the absorption attributed to a "background" concentration; d_s, the fraction covarying with phytoplankton absorption; and S, the slope of the decay of $a_{cdom+det}(\lambda)$ with wavelength. Values of D_0 were selected to represent environments ranging from oligotrophic oceanic waters to estuarine waters (based on *Kirk* [1994b]). The range of d_s was based on our absorption data from a variety of coastal waters (not shown), in which we compared measured values of the absorption coefficient by phytoplankton to measured values of the combined contribution of absorption by CDOM and detritus at 443 nm. Values for S vary over published ranges for CDOM absorption [e.g., *Carder et al.*, 1989; *Green and Blough*, 1994].

Changes in D_0 (Figure 11a) affected the relationship between $K_d(490)$ and $L_u(443)/L_u(550)$ slightly at low C, and changes in d_s (Figure 11b) hardly influenced the shape of
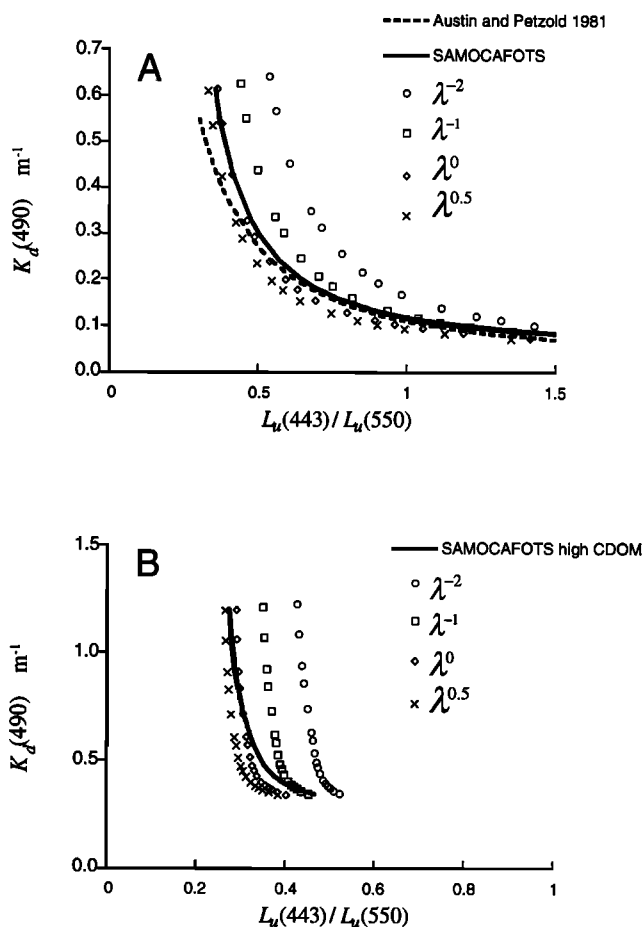
Figure 9. Sensitivity of (a) SAMOCAFOTS and (b) SAMOCAFOTS high CDOM to the wavelength dependence of the particle scattering coefficient (γ), varying as described in the legend. More negative exponents are associated with the importance of smaller particles. All the other parameters (packaging, pigment composition, and CDOM plus detrital absorption) are a function of C, as in SAMOCAFOTS. The empirical relationship by *Austin and Petzold* [1981] is plotted in Figure 9a for comparison.
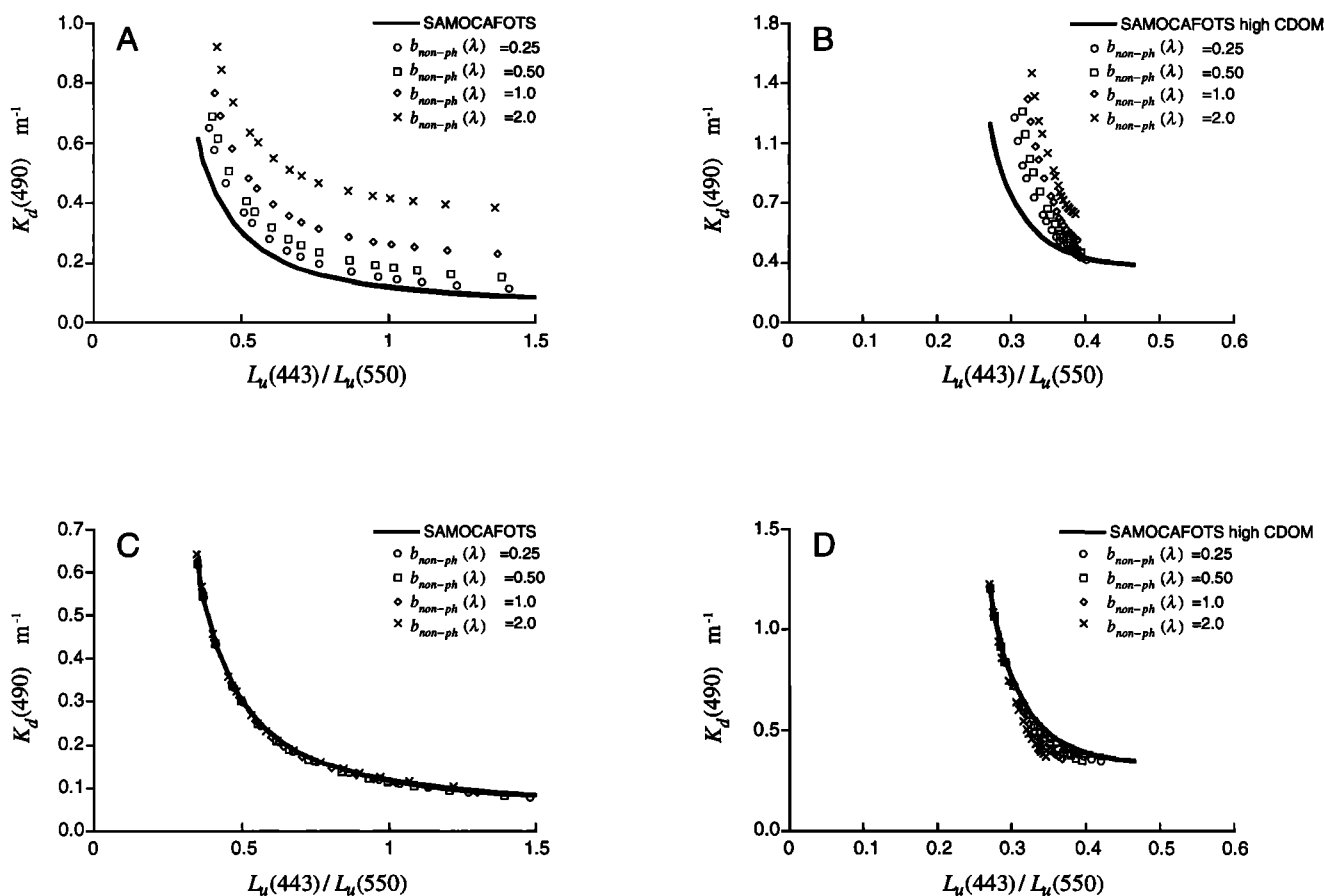
Figure 10. Influence of an additional input of particles simulated by their attenuation coefficient at 660 nm, $b_{non-ph}(660)$. (a and b) Increments of $b_{non-ph}(660)$, simulating the input of particles with backscattering ratio equal to 0.08, low absorption coefficient and dependency of λ^{-1} for the scattering coefficient, for SAMOCAFOTS and SAMOCAFOTS high CDOM, respectively. (c and d) Same as Figures 10a and 10b, only for input of particles with backscattering ratio of 0.01 and no spectral dependency for the scattering coefficient.

the relationship. This may be one of the reasons why the empirical relationship of Austin and Petzold [1981] has been shown to hold in more turbid environments [Cullen et al., 1994]. In fact, if we were to extrapolate SAMOCAFOTS to very high (and unreasonable) C, and the empirical relationships to lower values of $L_u(443)/L_u(550)$, the curves would explain from 40 to 60% of the variability of the data with high $K_d(490)$. In other words, despite the variability in $a_{cdom+det}(\lambda)$ in Bedford Basin (see Figure 6), empirical relationships can still predict $K_d(490)$ with some degree of accuracy.

The effect of increasing $a_{cdom+det}(\lambda)$ is to reduce the overall sensitivity of the radiance ratios to distinguish between the different levels of C, as anticipated [Gordon et al., 1983, and references therein] and verified in the field [Hochman et al., 1995]. Figures 11c and 11d show the effects of varying D_0 and d_s, respectively, on the ratio of upwelling radiance at 490 to that at 550 nm and the resulting changes in C retrieved using the SeaWiFS algorithm [O'Reilly et al., 1998]. Changes in d_s affected the results modestly (less than 40%); however, changes in D_0 resulted in an overestimation of the retrieved C by a factor of more than 10 when in situ C is low, and by a factor of 2 when in situ C is high. The attenuation coefficient remained sensitive to changes in C at

all concentrations of $a_{cdom+det}(\lambda)$ (Figures 11e and 11f) but will respond to both D_0 and d_s in a similar manner as $L_u(443)/L_u(550)$ does. Because in our parameterization the relationship between $a_{cdom+det}$ and a_{ph} is linear, it is not surprising that the effects of both D_0 and d_s on $L_u(443)/L_u(550)$ and $K_d(490)$ are proportional to one another, and therefore the form of original relationship is maintained.

So far, we have assessed the influence of CDOM plus detrital absorption by varying the total amount while keeping the spectral shape constant. The shape is expected to change depending on the composition and origin of CDOM, which is manifested by changes in the slope S [Carder et al., 1989]. Because of that, S could be expected to vary seasonally. In addition, in waters such as Bedford Basin, the variability in S could follow a range of different timescales, associated with tidal and wind mixing as well as river outflow and precipitation rates. The sensitivity of SAMOCAFOTS to S (Figure 12) shows that it can influence significantly the relationship when $a_{cdom+det}(\lambda)$ is high. The range of variability around the central tendency explained by SAMOCAFOTS high CDOM (Figure 12b) is consistent with the range of variability found during our time series experiment in Bedford Basin, suggesting that models should
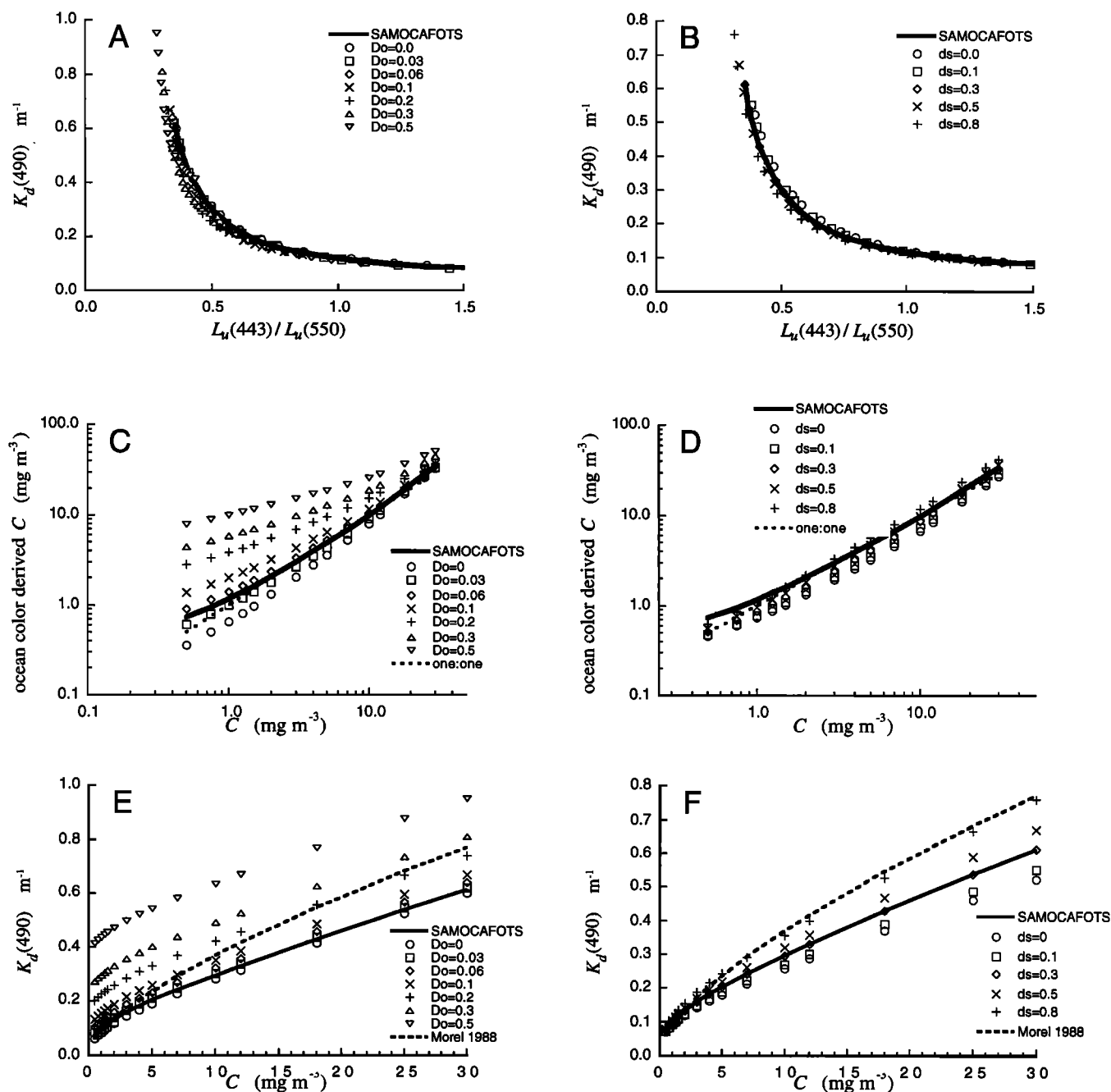
Figure 11. (a) Sensitivity analysis of SAMOCAFOTS to changes in D_0, the absorption by the background concentration of CDOM and detritus. Values of D_0 represent CDOM absorption at 443 nm within the ranges found from oligotrophic to estuarine waters. (b) Sensitivity to d_s, the slope of the assumed linear relationship between phytoplankton and CDOM and detritus absorption. Values of d_s represent ranges found in our database for absorption at 443 nm in a variety of coastal waters. (c and d) Same as in Figures 11a and 11b, only for the relationship between $L_u(490)/L_u(550)$ which was parameterized as in (26) with the relevant parameters modified from 443 to 490 nm and C. (e and f) Same as in Figures 11a and 11b, only for the relationship between $K_d(490)$ and C. The empirical model by *Morel* [1988] is plotted for comparison.

incorporate terms to account for the variability in S for water bodies in which CDOM is an important contributor to total absorption.

7. Summary and Conclusions

We constructed a semi-analytical model to explore the effects of diverse optical components on the relationship between upwelling radiance ratios and diffuse attenuation. The model was based on well described, fundamental sources of optical variability in the ocean. We parameterized optical properties as functions of C, consistent with observations from the field, reconciled with theoretical and laboratory-derived optical relationships. Although C is a poor descriptor of phytoplankton biomass [*Cullen*, 1982], the construction of a general (or "expected") relationship as a function of C
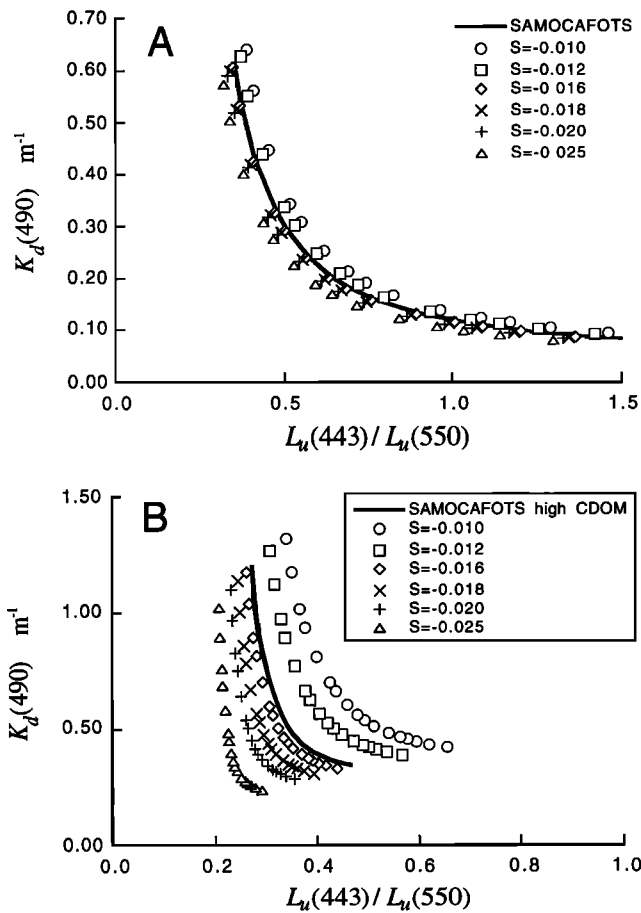
Figure 12. Sensitivity analysis of SAMOCAFOTS to changes in S, the slope of the decrease of CDOM plus detrital absorption with wavelength. Values of S represent ranges found in the literature and in our database.

allowed us to develop more mechanistic approaches to interpret changes in phytoplankton optical properties as a function of trophic status [e.g., *Yentsch and Phinney*, 1989]. In addition, analysis and interpretation of deviations from the expected trend can be useful tools [e.g., *Morel*, 1997].

The resulting general relationship between $K_d(490)$ and $L_u(443)/L_u(550)$ reproduced well both empirical models and independent bio-optical data from a variety of environments. The individual parameterizations of diffuse attenuation and radiance ratios also agreed well with patterns in data from the field. Our model reconciles relationships between inherent and apparent optical properties, as well as theoretical, laboratory, and field observations. The agreement between statistical

models and the semi-analytical expressions was above 80% for $L_u(443)/L_u(550)$ above 0.5. The parameterization of phytoplankton absorption can be modified to include a range of phytoplankton communities for a given value of C.

Variability around the central tendency explained by the general model was modeled by varying the original relationship between the input parameters and C. The estimated deviations from the general model could be related to the variability observed in the field measurements. Substantial deviations were produced by (1) changes in packaging at high accessory pigment concentration, (2) changes in the spectral shape of the scattering coefficient (implying changes in the size distribution of the particles and also different types of particles) in environments where CDOM and detrital absorption is important, and (3) variability in nonphytoplanktonic absorption, particularly changes in S, the slope of the decrease in absorption with wavelength, in environments expected to have a large contribution of CDOM and/or detrital absorption. Although with the set of wave bands used in this analysis it is difficult to distinguish among these effects, we speculate that packaging and high accessory pigment concentration explain in large part the deviations found during a red tide event (BBS93), because during this experiment, absorption by CDOM remained relatively consistent. These deviations could be applied in monitoring such events using simple passive optical instruments [*Cullen et al.*, 1997]. Our analyses suggest that SAMOCAFOTS-like relationships could be constructed to discriminate rough features among different phytoplankton communities (i.e., packaging), given a set of optimized wavelengths which minimizes the influence of CDOM and detrital absorption. Algorithms using two or more radiance ratios (with SeaWiFS wavelengths) to estimate chlorophyll concentrations in waters with CDOM and detrital influence are being developed and tested [e.g., *Aiken et al.*, 1995, and references therein].

Another important point can be made regarding the predictive skills of the semi-analytical relationship compared to the empirical ones: in the independent data set presented in this paper, the forecast skill of $K_d(490)$ from $L_u(443)/L_u(550)$ was about the same using our model as with the empirical relationships. This is not unexpected, as both the general semi-analytical and empirical equations represent general trends or averages of the variability in optical properties by phytoplankton and other components. The main goal of expressing optical properties through semi-analytical expressions, rather than improving their statistical forecast skill, is to produce tools to understand quantitatively the factors that influence these properties. Once these factors are defined, some forecast skill improvement can be made if independent and concurrent optical measurements are made to account for first-order deviations from the general trend.

Notation

$a(\lambda)$	total absorption coefficient, m^{-1}.
$a_{cdom}(\lambda)$	absorption coefficient due to CDOM, m^{-1}.
$a_{cdom+det}(\lambda)$	absorption coefficient due to combined effects of CDOM and detritus, m^{-1}.
$a_{ph}(\lambda)$	absorption coefficient for phytoplankton, m^{-1}.
$a_w(\lambda)$	absorption coefficient for pure water, m^{-1}.
$a_{ph}^*(\lambda)$	phytoplankton specific absorption coefficient, m^2 $mgChl^{-1}$.
$a_{sol}^*(\lambda)$	pigment cellular solution specific absorption coefficient, m^2 $mgChl^{-1}$.

$b(\lambda)$	total scattering coefficient, m^{-1}.
$b_{ph+det}(\lambda)$	scattering coefficient for particles, m^{-1}.
$b_{non+ph}(\lambda)$	scattering coefficient for additional particles, m^{-1}.
$b_b(\lambda)$	total backscattering coefficient, m^{-1}.
$\tilde{b}b_{ph+det}(\lambda)$	backscattering ratio for the particle assemblage, dimensionless.
C	chlorophyll a plus pheopigment concentration, $mg\ m^{-3}$.
c_i	intracellular pigment concentration, $mg\ m^{-3}$.
d	equivalent spherical diameter, m.
D_0	intercept of the linear relationship between a_{ph} and $a_{cdom-det}$ at 443 nm, m^{-1}.
d_s	slope of the linear relationship between a_{ph} and $a_{cdom-det}$ at 443 nm, dimensionless.
$E_u(\lambda), E_d(\lambda)$	upwelling and downwelling irradiance, $W\ m^{-2}\ nm^{-1}$.
$E_{0d}(\lambda)$	downwelling scalar irradiance, $W\ m^{-2}\ nm^{-1}$.
$f(\lambda)$	parameter that relates reflectance to the ratio between backscattering and absorption, dimensionless.
$K_{d_w}(\lambda)$	diffuse attenuation coefficient by water, m^{-1}.
$K_d(\lambda)$	diffuse attenuation coefficient for downwelling irradiance, m^{-1}.
$L_u(\lambda)$	upwelling radiance, $W\ m^{-2}\ nm^{-1}\ sr^{-1}$.
λ	wavelength, nm.
M	factor from (4), dimensionless.
γ	spectral dependency of $b_{ph+det}(\lambda)$, dimensionless.
γ_{non-ph}	spectral dependency of $b_{non+ph}(\lambda)$, dimensionless.
$\rho'(\lambda)$	particle optical thickness, dimensionless.
$Q(\lambda)$	ratio of upwelling irradiance to upwelling nadir radiance, sr.
$Q_a(\lambda)$	efficiency coefficient for absorption, dimensionless.
$Q_a^*(\lambda)$	packaging effect coefficient, dimensionless.
RSC	estimated C from radiance ratio algorithms, $mg\ m^{-3}$.
$R(\lambda)$	irradiance reflectance, dimensionless.
S	slope of the exponential decrease of $a_{cdom-det}$ with wavelength, nm^{-1}.
$\bar{\mu}_d$	average cosine for downwelling irradiance, dimensionless.

References

Aarup, T., N. Holt, and N.K. Højerslev, Optical measurements in the North Sea-Baltic transition zone, III, Statistical analysis of bio-optical data from the Eastern North Sea, the Skaterrak and the Kattegat, *Cont. Shelf Res.*, *16*(10), 1355-1377, 1996.

Agusti, S., Allometric scaling of light absorption and scattering by phytoplankton cells, *Can. J. Fish. Aquat. Sci.*, *48*, 763-768, 1991.

Ahn, Y.H., A. Bricaud, and A. Morel, Light backscattering efficiency and related properties of some phytoplankters, *Deep Sea Res.*, *39* (11-12A), 1835-1855, 1992.

Aiken, J., G.F. Moore, and P.M. Holligan, Remote sensing of oceanic biology in relation to global climate change, *J. Phycol.*, *128*(5), 579-590, 1992.

Aiken, J., G.F. Moore, C.C. Trees, S.B. Hooker, and D.K. Clark, The SeaWiFS CZCS-type pigment algorithm, edited by S.B. Hooker and E.R. Firestone, 34 pp; NASA Goddard Space Flight Cent., Greenbelt, Md., 1995.

Austin, R.W., and T.J. Petzold, Remote sensing of the diffuse attenuation coefficient of sea water using the Coastal Zone Color Scanner, in *Oceanography from Space*, edited by J.R.F. Gower, pp. 239-256, Plenum, New York, 1981.

Austin, R.W., and T.J. Petzold, Spectral dependence of the diffuse attenuation coefficient of light in ocean waters, *Opt. Eng.*, *25*, 471-479, 1986.

Babin, M., J.C. Therriault, L. Legendre, and A. Condal, Variations in the specific absorption coefficient for natural phytoplankton assemblages: Impact on estimates of primary production, *Limnol. Oceanogr.*, *38*(1), 154-177, 1993.

Bidigare, R.R., M.E. Ondrusek, J.H. Morrow, and D.A. Kiefer, In vivo absorption properties of algal pigments, *Opt. Eng.*, *1302*, 290-302, 1990.

Bishop, Y.M.M., S.E. Fienberg, and P.W. Holland, *Discrete Multivariate Analysis: Theory and Practice*, 557 pp., MIT Press, Cambridge, Mass, 1975.

Bricaud, A., and A. Morel, Light attenuation and scattering by phytoplankton cells: A theoretical modeling, *Appl. Opt.*, *25*(4), 571-580, 1986.

Bricaud, A., and D. Stramski, Spectral absorption coefficients of living phytoplankton and nonalgal biogenous matter: A comparison between the Peru upwelling area and the Sargasso Sea, *Limnol. Oceanogr.*, *35*(3), 562-582, 1990.

Bricaud, A., A. Morel, and L. Prieur, Absorption by dissolved organic matter of the sea (yellow substance) in the UV and visible domains, *Limnol. Oceanogr.*, *26*(1), 43-53, 1981.

Bricaud, A., A. Morel, and L. Prieur, Optical efficiency factors of some phytoplankters, *Limnol. Oceanogr.*, *28*(5), 816-832, 1983.

Bricaud, A., M. Babin, A. Morel, and H. Claustre, Variability in the chlorophyll-specific absorption coefficients of natural phytoplankton: Analysis and parameterization, *J. Geophys. Res.*, *100*, 13,321-13,332, 1995.

Bukata, R.P., J.E. Bruton, and J.H. Jerome, Use of chromaticity in remote measurements of water quality, *Remote Sens. Environ.*, *13*, 161-177, 1983.

Bukata, R.P., J.H. Jerome, K.Y. Kondratyev, and D.V. Pozdnyakov, *Optical Properties and Remote Sensing of Inland and Coastal Waters*, 362 pp., CRC Press, Boca Raton, Fla., 1995.

Campbell, J.W., The lognormal distribution as a model for bio-optical variability in the sea, *J. Geophys. Res.*, *100*, 13,237-13,254, 1995.

Carder, K.L., R.G. Steward, G.R. Harvey, and P.B. Ortner, Marine humic and fulvic acids: Their effects on remote sensing of ocean chlorophyll, *Limnol. Oceanogr.*, *34*(1), 68-81, 1989.

Chisholm, S.W., R.J. Olson, E.R. Zettler, R. Goericke, J.B. Waterbury, and N.A. Welschmeyer, A novel free-living prochlorophyte abundant in the oceanic euphotic zone, *Nature*, *334*, 340-343, 1988.

Ciotti, A.M., J.J. Cullen, C.S. Roesler, and M.R. Lewis, The influence of phytoplankton size structure on the spectral attenuation coefficient in the upper ocean, Ocean Opt. 13 Proc., *SPIE Int. Soc. Opt. Eng.*, *2963*, 380-385, 1996.

Claustre, H., The trophic status of various oceanic provinces as revealed by phytoplankton pigment signatures, *Limnol. Oceanogr.*, *39*(5), 1206-1210, 1994.

Cullen, J.J., The deep chlorophyll maximum: comparing vertical profiles of chlorophyll a, *Can. J. Fish. Aquat. Sci.*, *39*(5), 791-803, 1982.

Cullen, J.J., A.M. Ciotti, and M.R. Lewis, Observing biologically induced optical variability in coastal waters, Ocean Opt. 12, Proc. SPIE Int. Soc. Opt. Eng., *2258*, 105-115, 1994.

Cullen, J.J., A.M. Ciotti, R.F. Davis, and M.R. Lewis, Optical detection and assessment of algal blooms, *Limnol. Oceanogr.*, *42*(5), 1223-1239, 1997.

Duysens, L.N.M., The flattening of the absorption spectrum of suspensions as compared to that of solutions, *Biochim. Biophys. Acta*, *19*, 1-12, 1956.

Eppley, R.W., W.G. Harrison, S.W. Chisholm, and E. Stewart, Particulate organic matter in surface waters off southern California and its relationship to phytoplankton, *J. Mar. Res.*, *35*(4), 671-696, 1977.

Gieskes, W.W.C., G.W. Kraay, A. Nontji, D. Setiapermana, and A. B. Sutomo, Monsoonal alternation of a mixed and a layered structure in the phytoplankton of the euphotic zone of the Banda Sea (Indonesia): A mathematical analysis of algal pigment fingerprints, *Neth. J. Sea Res.*, *22*(2), 123-137, 1988.

Gordon, H.R., and A.Y. Morel, *Remote Assessment of Ocean Color for Interpretation of Visible Satellite Imagery: A Review*, 114 pp., Springer-Verlag, New York, 1983.

Gordon, H.R., O.B. Brown, and M.M. Jacobs, Computed relationships between the inherent and apparent optical properties of a flat homogeneous ocean, *Appl. Opt.*, *14*, 417-427, 1975.

Gordon, H.R., D.K. Clark, J.W. Brown, O.B. Brown, R.H. Evans, and W.W. Broenkow, Phytoplankton pigment concentrations in the Middle Atlantic Bight: Comparison between ship determinations and Coastal Zone Color Scanner estimates, *Appl. Opt.*, *22*, 20-36, 1983.

Gordon, H.R., O.B. Brown, R.H. Evans, J.W. Brown, R.C. Smith, K.S. Baker, and D.K. Clark, A semianalytic radiance model of ocean color, *J. Geophys. Res.*, *93*, 10,909-10,924, 1988.

Green, S.A., and N.V. Blough, Optical absorption and fluorescence properties of chromophoric dissolved organic matter in natural waters, *Limnol. Oceanogr.*, *39*(8), 1903-1916, 1994.

Gregg, W.W., and K.L. Carder, A simple spectral solar irradiance model for cloudless maritime atmospheres, *Limnol. Oceanogr.*, *35*(8), 1657-1675, 1990.

Hochman, H.T., J.J.Walsh, and K.L.Carder, Analysis of ocean color components within stratified and well-mixed waters of the western English Channel, *J. Geophy. Res.*, *100*, 10,777-10,787, 1995.

Hoepffner, N., and S. Sathyendranath, Effect of pigment composition on absorption properties of phytoplankton, *Mar. Ecol. Prog. Ser.*, *73*, 11-23, 1991.

Johnsen, G., and E. Sakshaug, Bio-optical characteristics and photoadaptive responses in the toxic and bloom-forming dinoflagellates *Gyrodinium aureolum*, *Gymnodinium galatheanum*, and two strains of *Prorocentrum minimum*, *J. Phycol.*, *29*(5), 627-642, 1993.

Johnsen, G., O. Samset, L. Granskog, and E. Sakshaug, In vivo absorption characteristics in 10 classes of bloom-forming phytoplankton: Taxonomic characteristics and responses to photoadaptation by means of discriminant and HPLC analysis, *Mar. Ecol. Prog. Ser.*, *105*, 149-157, 1994.

Kirk, J.T.O., Characteristics of the light field in highly turbid waters: A Monte Carlo study, *Limnol. Oceanogr.*, *39*(3), 702-706, 1994a.

Kirk, J.T.O., *Light and Photosynthesis in Aquatic Ecosystems*, 509 pp., Cambridge University Press, New York, 1994b.

Lewis, M.R., and J.J. Cullen, From cells to the ocean: Satellite ocean color, in *Particle Analysis in Oceanography*, edited by S. Demers, pp. 325-337, Springer-Verlag, New York, 1991.

Lewis, M.R., M.E. Carr, G.C. Feldman, W. Esais, and C. McClain, Influence of penetrating solar radiation on the heat budget of the equatorial Pacific Ocean, *Nature*, *347*, 543-545, 1990.

Loisel, H., and A. Morel, Light scattering and chlorophyll concentration in case I waters: A re-examination, *Limnol. Oceanogr.*, 43(5), 847-858, 1998.

Lutz, V.A., S. Sathyendranath, and E.J.H. Head, Absorption coefficient of phytoplankton: Regional variations in the North Atlantic, *Mar. Ecol. Prog. Ser.*, *135*, 197-213, 1996.

MacIntyre, J.G., J.J. Cullen, and A.D. Cembella, Vertical migration, nutrition and toxicity in the dinoflagellate *Alexandrium tamarense*, *Mar. Ecol. Progr. Ser.*, *148*, 201-216, 1997.

Malone, T.C., Algal size, in *The Physiological Ecology of Phytoplankton*, edited by I. Morris, pp. 433-463, Univ. of Calif. Press, Berkeley, 1980.

Miller, W.L., Recent advances in the photochemistry of natural dissolved organic matter, in *Aquatic and Surface Photochemistry*, edited by G.R. Heltz, pp. 111-127, A. F. Lewis, New York, 1994.

Mitchell, B.G., Predictive bio-optical relationships for polar oceans and marginal ice zones, *J. Mar. Syst.*, *3*, 1-2, 1992.

Mobley, C.D., *Light and Water: Radiative Transfer in Natural Waters*, 592 pp., Academic, San Diego, Calif., 1994.

Morel, A., Optical modeling of the upper ocean in relation to its biogenous matter content (Case I waters), *J. Geophy. Res.*, *93*, 10,749-10,768, 1988.

Morel, A., Optics from the single cell to the mesoscale, in *Ocean Optics*, edited by R.W. Spinrad, K.L. Carder, and M.J. Perry, pp. 93-106, Oxford Univ. Press, New York, 1994.

Morel, A., Consequences of a *Synechococcus* bloom upon the optical properties of oceanic (Case I) waters, *Limnol. Oceanogr.*, *42*(8), 1746-1754, 1997.

Morel, A., and Y.H. Ahn, Optics of heterotrophic nanoflagellates and ciliates: A tentative assessment of their scattering role in oceanic waters compared to those of bacterial and algal cells, *J. Mar. Res.*, *49*(1), 177-202, 1991.

Morel, A., and A. Bricaud, Theoretical results concerning light absorption in a discrete medium, and application to specific absorption of phytoplankton, *Deep Sea Res.*, *28A*(11), 1375-1393, 1981.

Morel, A., and A. Bricaud, Inherent properties of algal cells including picoplankton: Theoretical and experimental results, in *Photosynthetic Picoplankton*, edited by T. Platt and W.K.W. Li, *Can. Bull. Fish. Aquat. Sci.*, *214*, 521-559, 1986,

Morel, A., and B. Gentili, Diffuse reflectance of oceanic waters, 2, Bidirectional aspects, *Appl. Opt.*, *32*(33), 6864-6872, 1993.

Morel, A., and B. Gentili, Diffuse reflectance of oceanic waters, 3, Implication of bidirectionality for the remote-sensing problem, *Appl. Opt.*, *35*(24), 4850-4862, 1996.

Morel, A., and L. Prieur, Analysis of variations in ocean color, *Limnol. Oceanogr.*, 22(4), 709-722, 1977.

Morel, A., Y. Ahn, F. Partensky, D. Vaulot, and H. Claustre, *Prochlorococcus* and *Synechococcus*: A comparative study of their optical properties in relation to their size and pigmentation, *J. Mar. Res.*, *5*(3), 617-649, 1993.

Mueller, J.L., and C.C. Trees, Revised SeaWiFS prelaunch algorithm for the diffuse attenuation coefficient K(490), in *Case Studies for SeaWiFS Calibration and Validation, Part 4.*, edited by E. Yeh, et al., *NASA Tech. Memo.*, *104566*, 18-21, 1997.

Nelson, N.B., and B.B. Prézelin, Chromatic light effects and physiological modeling of absorption properties of *Heterocapsa pygmaea* (= *Glenodinium* sp.), *Mar. Ecol. Prog. Ser.*, *63*, 37-40, 1990.

Nelson, N.B., B.B. Prézelin, and R.R. Bidigare, Phytoplankton light absorption and the package effect in California coastal waters, *Mar. Ecol. Prog. Ser.*, *94*, 217-227, 1993.

O'Reilly, J.E., S. Maritorena, B.G. Mitchell, D.A. Siegel, K.L. Carder, S.A. Garver, and C.R. McClain, Ocean color chlorophyll algorithms for SeaWiFS, *J. Geophys. Res.*, in press, 1998.

Platt, T., S. Sathyendranath, C.M. Caverhill, and M.R. Lewis, Oceanic primary production and available light: Further algorithms for remote sensing, *Deep Sea Res.*, *35*, 855-879, 1988.

Pope, R.M., and E.S. Fry, Absorption spectrum (380-700 nm) of pure water; II, Integrating cavity measurements, *Appl. Opt.*, *36*, 8710-8723, 1997.

Preisendorfer, R.W., Application of radiative transfer theory to light measurements in the sea, *Monogr. 10*, pp. 11-30, *Int. Union of Geod. and Geophys. Paris*, 1961.

Roesler, C.S., and M.J. Perry, In situ phytoplankton absorption, fluorescence emission, and particulate backscattering spectra determined from reflectance, *J. Geophys. Res.*, *100*, 13,279-13,294, 1995.

Roesler, C.S., M.J. Perry, and K.L. Carder, Modeling in situ phytoplankton absorption from total absorption spectra in productive inland waters, *Limnol. Oceanogr.*, *34*, 1510-1523, 1989.

Sathyendranath, S., and T. Platt, The spectral irradiance field at the surface and in the interior of the ocean: A model for applications in oceanography and remote sensing, *J. Geophys. Res.*, *93*, 9270-9280, 1988.

Sathyendranath, S., L. Lazzara, and L. Prieur, Variations in the spectral values of specific absorption of phytoplankton, *Limmol. Oceanogr.*, *32*(2), 403-415, 1987.

Sathyendranath, S., L. Prieur, and A. Morel, A three-component model of ocean colour and its application to remote sensing of phytoplankton pigments in coastal waters, *Int. J. Remote Sens.*, *10*(8), 1373-1394, 1989.

SooHoo, J.B., and D.A. Kiefer, Vertical distribution of phaeopigments, 2, Rates of production and kinetics of photooxidation, *Deep Sea Res.*, *29*(12A), 1553-1563, 1982.

Sosik, H.M., and B.G. Mitchell, Effects of temperature on growth, light absorption, and quantum yield in *Dunaliella tertiolecta* (Chlorophyceae), *J. Phycol.*, *30*(5), 833-840, 1994.

Sosik, H.M., and B.G. Mitchell, Light absorption by phytoplankton, photosynthetic pigments and detritus in the California Current System, *Deep Sea Res.*, *42*(10), 1717-1748, 1995.

Stramski, D., Gas microbubbles: An assessment of their significance to light scattering in quiescent sea, *Ocean Opt. 12, Proc. SPIE Int. Soc. Opt. Eng.*, 2258, 704-710, 1994.

Stramski, D., and D.A. Kiefer, Light scattering by microorganisms in the open ocean, *Prog. Oceanogr.*, *28*, 343-383, 1991.

Stramski, D., and R.A. Reynolds, Diel variations in the optical properties of a marine diatom, *Limnol. Oceanogr.*, *38*(7), 1347-1364, 1993.

Stramski, D., G. Rosenberg, and L. Legendre, Photosynthetic and optical properties of the marine chlorophyte *Dunaliella tertiolecta* grown under fluctuating light caused by surface-wave focusing, *Mar. Ecol. Prog. Ser.*, *115*, 363-372, 1993.

Stuart, V., S. Sathyendranath, T. Platt, H. Maass, and B.D. Irwin, Pigments and species composition of natural phytoplankton populations: Effects on the absorption spectra, *J. Plankton Res.*, *20*(2), 187-217, 1998.

Subramaniam, A., and E.J. Carpenter, An empirically derived protocol for the detection of blooms of the marine cyanobacterium *Trichodesmium* using CZCS imagery, *Int. J. Remote Sens.*, *15*(8), 1559-1569, 1994.

Ulloa, O., S. Sathyendranath, and T. Platt, Effect of the particle size distribution on the backscattering ratio in seawater, *Appl. Opt.*, *33*, 7070-7077, 1994.

van de Hulst, H.C., *Light Scattering by Small Particles*, John Wiley, New York, 1957.

Yentsch, C.S., and D.A. Phinney, A bridge between ocean optics and microbial ecology, *Limnol. Oceanogr.*, *34*(8), 1694-1705, 1989.

Zhang, X., M.R. Lewis, and B. Johnson, The influence of bubbles on scattering of light in the ocean, *Appl. Opt.*, *37*(27), 6525-6536, 1998.

A. M. Ciotti (corresponding author), J. J. Cullen, and M. R. Lewis, Centre for Environmental Observation Technology and Research, Department of Oceanography, Dalhousie University, Halifax, N.S., Canada B3H 4J1. (e-mail: aurea@raptor.ocean.dal.ca)